



**US Army Corps
of Engineers**

DREDGING RESEARCH PROGRAM

MISCELLANEOUS PAPER DRP-94-1

**CHL
LIBRARY**

DISPERSION ANALYSIS OF CHARLESTON, SOUTH CAROLINA, OCEAN DREDGED MATERIAL DISPOSAL SITE

by

Norman W. Scheffner, James R. Tallent

DEPARTMENT OF THE ARMY

Waterways Experiment Station, Corps of Engineers
3909 Halls Ferry Road, Vicksburg, Mississippi 39180-6199



March 1994

Final Report

Approved For Public Release; Distribution Is Unlimited

Prepared for US Army Engineer District, Charleston
Charleston, South Carolina 29402-0919

The Dredging Research Program (DRP) is a seven-year program of the US Army Corps of Engineers. DRP research is managed in these five technical areas:

Area 1 - Analysis of Dredged Material Placed in Open Water

Area 2 - Material Properties Related to Navigation and Dredging

Area 3 - Dredge Plant Equipment and Systems Processes

Area 4 - Vessel Positioning, Survey Controls, and Dredge Monitoring Systems

Area 5 - Management of Dredging Projects

Destroy this report when no longer needed. Do not return
it to the originator.

The contents of this report are not to be used for
advertising, publication, or promotional purposes.
Citation of trade names does not constitute an official
endorsement or approval of the use of such
commercial products.



US Army Corps
of Engineers
Waterways Experiment
Station

Dredging Research Program Report Summary



Dispersion Analysis of Charleston, South Carolina, Ocean Dredged Material Disposal Site (MP DRP-94-1)

ISSUE: The site designated for the offshore disposal of material dredged from the Charleston, SC, harbor is located southeast of the harbor entrance. Historically, materials deposited in the Ocean Dredged Material Disposal Site (ODMDS) have been predominately fine-grained sand with some silt and clay. Because the material from a proposed inner harbor-deepening project contained a higher percentage of silt and clay, the Environmental Protection Agency (EPA) conducted a video survey to determine if the ODMDS contained ecologically sensitive areas that might be affected by the disposal of the finer-grained material. The EPA identified areas of live bottom habitat within the Charleston ODMDS.

RESEARCH: The dispersive characteristics of the disposal site were investigated as a function of the local wave and current environment. Site-specific wave and current information was used for the boundary-condition development for numerical modeling of the short-term effects of the disposal operation as well as the long-term behavior of the disposal mound. Results of this study contribute to the body of knowledge from similar site-

characterization studies and to the credibility of numerical modeling efforts.

SUMMARY: Short-term numerical simulations indicated that even when worst-case currents are reef directed, the finer-grained dredged material does not appear to pose a threat if the disposal location is situated at least 1.5 miles from the bottom habitat. Long-term dredged material mound movement is relatively small under normal conditions. However, storm-induced currents may cause erosion and transport of material that could pose a threat to the coral reefs if conditions are severe and storm durations are significant unless disposal mounds are located a reasonable distance to the northeast of the area of bottom habitat.

AVAILABILITY OF REPORT: The report is available through the Interlibrary Loan Service from the U.S. Army Engineer Waterways Experiment Station (WES) Library, telephone number (601) 634-2355. National Technical Information Service (NTIS) report numbers may be requested from WES Librarians.

To purchase a copy of the report, call NTIS at (703) 487-4780.

About the Authors: Drs. Norman W. Scheffner and James R. Tallent are members of the Coastal Processes Branch, Research Division, Coastal Engineering Research Center, WES

Point of Contact: Dr. Scheffner, Principal Investigator for the work unit.

For further information about the DRP, contact Mr. E. Clark McNair, Jr., Manager, DRP, at (601) 634-2070.

Dispersion Analysis of Charleston, South Carolina, Ocean Dredged Material Disposal Site

by Norman W. Scheffner, James R. Tallent

U.S. Army Corps of Engineers
Waterways Experiment Station
3909 Halls Ferry Road
Vicksburg, MS 39180-6199

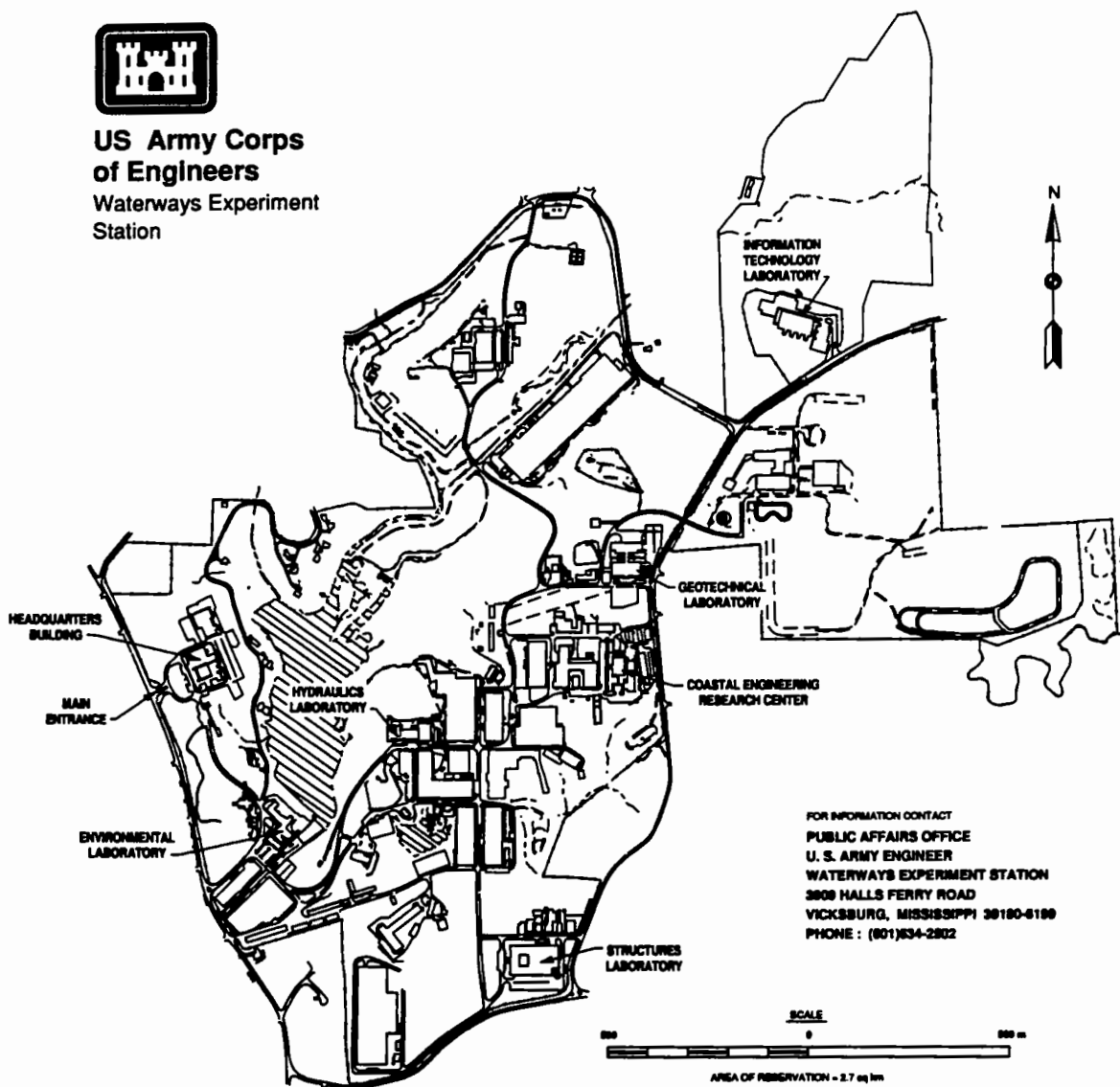
Final report

Approved for public release; distribution is unlimited

Prepared for U.S. Army Engineer District, Charleston
Charleston, South Carolina 29402-0919



**US Army Corps
of Engineers**
Waterways Experiment
Station



Waterways Experiment Station Cataloging-In-Publication Data

Scheffner, Norman W.

Dispersion analysis of Charleston, South Carolina, ocean dredged material disposal site / by Norman W. Scheffner, James R. Tallent ; prepared for U.S. Army Engineer District, Charleston, South Carolina.

73 p. : ill. ; 28 cm. — (Miscellaneous paper ; DRP-94-1)

Includes bibliographic references.

1. Dredging — South Carolina. 2. Sediment transport — South Carolina. 3. Dredging spoil — South Carolina. I. Tallent, James R. II. United States. Army. Corps of Engineers. III. U.S. Army Engineer Waterways Experiment Station. IV. United States. Army. Corps of Engineers. Charleston District. V. Title. VI. Series: Miscellaneous paper (U.S. Army Engineer Waterways Experiment Station) ; DRP-94-1.

TA7 W34m no.DRP-94-1

PREFACE

The site designation methodology used in this report was developed at the Coastal Engineering Research Center (CERC) and the Hydraulics Laboratory, US Army Engineer Waterways Experiment Station (WES) by work units of Technical Area 1 (TA1), Analysis of Dredged Materials Disposal in Open Water, of the Dredging Research Program (DRP) of Headquarters, US Army Corps of Engineers (HQUSACE). Messrs. Robert Campbell and Glenn R. Drummond were DRP Chief and TA1 Technical Monitor from HQUSACE, respectively. Mr. E. Clark McNair, Jr., CERC, was DRP Program Manager and Dr. Lyndell Z. Hales, CERC, was Assistant Program Manager. Dr. Nicholas C. Kraus, Senior Scientist, Research Division (RD), CERC was Technical Manager for DRP TA1.

This report describes an investigation of the dispersion characteristics of the existing Charleston Ocean Dredged Material Disposal Site, located southeast of the entrance to Charleston Harbor. The study was conducted by CERC at the request of the US Army Engineer District (USAED), Charleston. Two sources of current measurements were used in the present analysis. The first source was data collected by the National Oceanic and Atmospheric Administration (NOAA) as a component of the Charleston Harbor Oceanography Project. Appreciation is extended to Drs. Henry Frey and Wayne L. Wilmot and Mr. Cary R. Wong, NOAA, for providing this information. The second source of data was provided by the US Environmental Protection Agency. Appreciation is extended to Mr. Philip J. Murphy, EPA, for making these data available. Appreciation is also extended to Mr. Steve J. Morrison, USAED, Charleston, for providing information and assistance crucial to the timely completion of this project.

Both phases of the numerical investigation and the final report were prepared by Drs. Norman W. Scheffner and James R. Tallent, Coastal Processes Branch (CPB), RD, CERC, WES.

Providing general supervision were Dr. James R. Houston and Mr. Charles C. Calhoun, Jr., Director and Assistant Director, respectively, CERC; direct supervision of the project was provided by Mr. H. Lee Butler, Chief, RD, and Mr. Bruce A. Ebersole, Chief, CPB.

At the time of publication of this report, Director of WES was Dr. Robert W. Whalin. Commander was COL Bruce K. Howard, EN.

For additional information on this work, contact Dr. Norman Scheffner, (601) 634-3220, or Mr. E. Clark McNair, Jr., at (601) 634-2070.

CONTENTS

	<u>Page</u>
PREFACE	1
LIST OF TABLES	4
LIST OF FIGURES	4
CONVERSION FACTORS, NON-SI TO SI (METRIC) UNITS OF MEASUREMENT . . .	6
SUMMARY	7
PART I: INTRODUCTION	9
Background	9
Objective	9
PART II: WAVE AND CURRENT BOUNDARY CONDITIONS	12
Wave Height, Period, and Direction Time Series	12
Depth-Averaged Current Time Series	17
PART III: SHORT-TERM MODELING	36
General	36
Input Data Requirements	37
Short-Term Model Simulations	41
Fine-Grained Disposal Site Analysis	41
Coarse-Grained Disposal Site Analysis	52
PART IV: LONG-TERM MODELING	60
General	60
Input Data Requirement	61
Long-Term Model Simulations	63
PART V: CONCLUSIONS	67
Prototype Data Analysis	67
Short-Term Analysis	68
Long-Term Analysis	68
Concluding Remarks	69
REFERENCES	70

LIST OF TABLES

<u>No.</u>		<u>Page</u>
1	Comparison of Wave Statistics	17
2	Summary Statistics of NOAA Current Data	19
3	Harmonic Analysis Summary	20
4	Harmonic Analysis Summary - EPA Data	34
5	Capacities and Dimensions of the Manhattan Class Dredge	38
6	Model Input Parameters and Coefficients	39
7	Fine-Grained Sediment Composition and Characteristics	40
8	Coarse-Grained Sediment Composition and Characteristics	40
9	Summary of the Computed Maximum Suspended Silt-Clay Concentration (Case 1)	48
10	Summary of the Computed Maximum Suspended Silt-Clay Concentration (Case 2)	48
11	Summary of the Computed Maximum Suspended Silt-Clay Concentration (Case 3)	55
12	Summary of the Computed Maximum Suspended Silt-Clay Concentration (Case 4)	55

LIST OF FIGURES

<u>No.</u>		<u>Page</u>
1	Charleston ODMDS location	10
2	WIS hindcast data station location	13
3	Simulated 1-year time series of wave height, period, and direction	14
4	WIS Station 69 time series for 1956	15
5	Probability histograms for simulated wave and 1956 WIS data	16
6	Station locations for current meter data	19
7	Station C-23 velocity component/directional data	22
8	Station C-24 velocity component/directional data	23
9	Station C-33 velocity component/directional data	24
10	Station C-34 velocity component/directional data	25
11	Current vector diagrams	26
12	Current vector relationships at Station C-24	27
13	Series 1 velocity component/directional data	30
14	Series 2 velocity component/directional data	31
15	Series 3 velocity component/directional data	32
16	Current vector diagrams	33
17	Simulated current time-series and vector diagram	35
18	Computational phases of the DIFID model	37
19	Suspended sediment cloud at 30-ft depth, 2,000 sec after disposal	43
20	Suspended sediment cloud at 30-ft depth, 4,000 sec after disposal	44
21	Suspended sediment cloud at 30-ft depth, 6,000 sec after disposal	45
22	Silt-clay concentration evolution relationships for the fine-grained site (Case 1)	46
23	Silt-clay concentration evolution relationships for the fine-grained site (Case 2)	47
24	Total deposition pattern for the fine-grained site (Case 1)	48

<u>No.</u>		<u>Page</u>
25	Total deposition pattern for the fine-grained site (Case 2) . .	49
26	Three-dimensional view of the fine-grained site deposition pattern (Case 1)	49
27	Three-dimensional view of the fine-grained site deposition pattern (Case 2)	50
28	Contour plot of the fine-grained site deposition pattern (Case 1)	50
29	Contour plot of the fine-grained site deposition pattern (Case 2)	51
30	Evolution of depth-averaged peak plume concentration for cases 1 and 2 of fine-grained material	51
31	Silt-clay concentration evolution relationships for the coarse-grained site (Case 3)	53
32	Silt-clay concentration evolution relationships for the coarse-grained site (Case 4)	54
33	Total deposition pattern for the coarse-grained site (Case 3) .	56
34	Total deposition pattern for the coarse-grained site (Case 4) .	56
35	Three-dimensional view of the coarse-grained site deposition pattern (Case 3)	57
36	Three-dimensional view of the coarse-grained site deposition pattern (Case 4)	57
37	Contour plot of the coarse-grained site deposition pattern (Case 3)	58
38	Contour plot of the coarse-grained site deposition pattern (Case 4)	58
39	Evolution of depth averaged peak plume concentration for Cases 3 and 4 of coarse-grained material	59
40	Sediment transport-velocity relationships for $D_{50} = 0.1000$ mm .	62
41	Sediment transport-velocity relationships for $D_{50} = 0.0625$ mm .	62
42	Idealized disposal mound perspective view	64
43	Idealized disposal mound contour map	64
44	Storm-event simulation perspective and contour map	66
45	Storm-event simulation mound axis migration history	66

CONVERSION FACTORS, NON-SI TO SI (METRIC)
UNITS OF MEASUREMENT

Non-SI units of measurement used in this report can be converted to SI
(metric) units as follows:

<u>Multiply</u>	<u>By</u>	<u>To Obtain</u>
cubic yards	0.7645549	cubic metres
degrees (angle)	0.01745329	radians
feet	0.3048	metres
miles (US nautical)	1.852	kilometres
miles (US statute)	1.609347	kilometres

SUMMARY

In this report the dispersion characteristics of dredged material placement operations at the Charleston, SC, Ocean Dredged Material Disposal Site (ODMDS) are investigated. The primary focus of the study is to determine if material deposited at the designated disposal site will migrate to the live coral reefs that were recently discovered within the boundaries of ODMDS. This study was conducted at the request of the U.S. Army Engineer District, Charleston.

A disposal site can be classified as dispersive or nondispersive depending on whether sediment is transported out of or remains within the designated limits of the site. The dredged material dispersion characteristics of the Charleston ODMDS were investigated in two phases, a short-term and long-term phase. In the short-term phase the potential effect of the actual barge disposal operation on the local environment was investigated. This phase of the study represents the initial minutes to hours following the disposal operation during which time the material is entrained and dispersed as it descends through the water column to be deposited on the ocean floor. Efforts were focused on modeling the time rate of change of suspended sediment concentration and the total sediment deposition pattern on the ocean bottom. In the second phase, the long-term analysis focuses on the extent and probable direction in which local waves and currents erode and transport the dredged material mound. The methodologies used to accomplish these goals are thoroughly discussed in the report.

Short-term numerical simulations were performed for worst-case wave and current conditions. Results include the water column spatial distribution of the sand and silt-clay components of the sediment load in the form of sediment concentration (parts per million) above the background level. Computational results indicate that a significant fraction of the sand and silt/clay materials falls rapidly to the ocean floor and does not impact regions beyond one-quarter mile from the point of disposal. However, a small amount of silt/clay material remains in the water column for several hours after the disposal operation. This cloud of suspended material is transported about 1 mile from the disposal point. The maximum thickness of the final deposition was approximately 0.5 ft, covering an approximate 700-ft-diameter area. Deposition is confined to this immediate area.

Results of the long-term simulations indicate that the mound is dispersive with respect to normal wave and tidal/circulation currents, with migration rates as large as 60 ft/month. Storm events significantly increased mound movement. The simulation of a moderate-intensity event with a 24-hr duration showed the mound migration to be approximately 155 ft.

Based on the findings of this report it is concluded that:

1) when the worst-case currents are reef directed, neither the sand nor the silt/clay materials appear to pose a threat if the disposal site is situated at least 1.5 miles from the reef, and 2) long-term dredged material mound movement is relatively small under normal conditions; however, storm-induced movement, which can be directed in virtually any direction, may pose a threat to the coral reefs if conditions are severe and storm durations are significant.

DISPERSION ANALYSIS OF CHARLESTON, SOUTH CAROLINA.
OCEAN DREDGED MATERIAL DISPOSAL SITE

PART I: INTRODUCTION

Background

1. The designated site for the offshore disposal of dredged material for Charleston, SC, is located southeast of the jettied entrance to Charleston Harbor, Figure 1. The approximately 5- by 9-km designated site has been in use for the disposal of dredged material since the mid-1970's. Historically, materials deposited at the site were predominately fine-grained sands with some silts and clays. The proposed inner harbor deepening project will require the disposal of approximately 3.0 million cubic yards* of material in the existing Ocean Dredged Material Disposal Site (ODMDS). Since the material from this project contains a higher percentage of fine-grained silts and clays than the original Charleston Harbor deepening project, an investigatory video survey was undertaken by the Environmental Protection Agency (EPA) to determine whether the site contained ecologically sensitive areas that may be affected by the disposal of fine-grained material. Results of that survey identified "extensive live bottom habitat areas within the Charleston ODMDS."** The purpose of this study is to use recently obtained prototype current data to quantify the local current patterns and magnitudes and to use these data to investigate the potential effect of the new disposal operation on the adjacent environmentally sensitive areas.

Objective

2. The objective of this study is to investigate the dispersive characteristics of the proposed site as a function of the local wave and current environment. In this manner, the potential effect of the disposal site on the

* A table for converting non-SI units of measurement to SI (metric) units is presented on page 5.

** Environmental Protection Agency, 14 February 1990, Memorandum Concerning the Location and Extent of Live Bottom Areas in the Charleston Ocean Dredged Material Disposal Site.

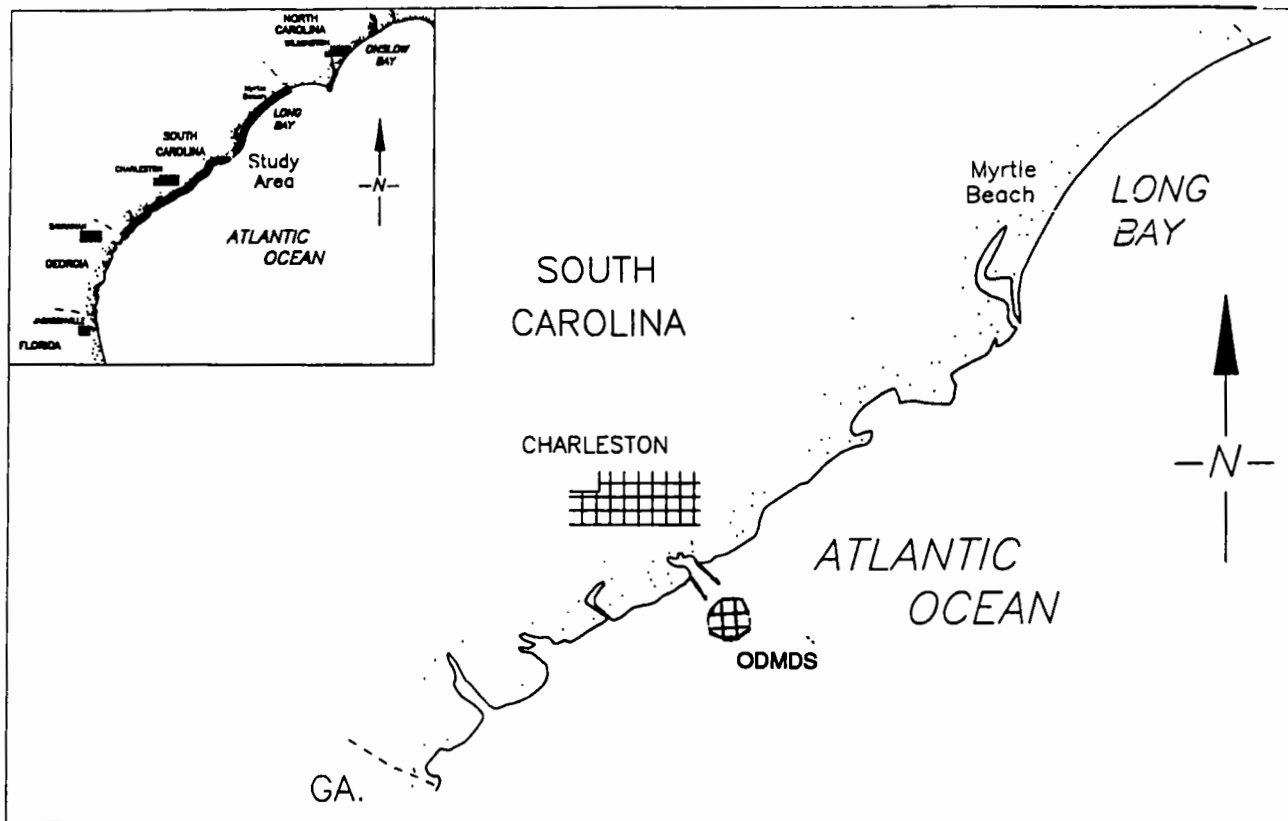


Figure 1. Charleston ODMDS location

underwater communities can be systematically investigated in a two-phase numerical-modeling-based approach. First, the short-term effects of the dredging operation are investigated to determine the time rate of change of suspended sediment concentration in the water column as the descending sediment plume disperses and is transported from the site by ambient currents. Additionally, the total sediment deposition pattern is computed to indicate the maximum spatial extent of deposition on the ocean bottom. The modeling of this short-term phase of the operation is performed by the Disposal from an Instantaneous Dump (DIFID) numerical model (Johnson 1990). This model computes the convective descent and dynamic collapse of the sediment following its release from the barge.

3. The second phase of the investigation examines the behavior of the sediment mound over long periods of time. Although it is recognized that the site is a dispersive one, this long-term analysis focuses on the extent and probable direction in which local waves and currents erode and transport deposited material from the sediment mound. These simulations are performed

with a coupled hydrodynamic, sediment transport, and bathymetry change model (Scheffner 1992 and in preparation) that computes mound stability as a function of mound composition and environmental forcings. Both modeling efforts require site-specific information, including waves, currents, bathymetry, sediment composition, and disposal methods.

4. A realistic analysis of the dispersion characteristics of the Charleston ODMDS can be made only if the computations are based on site-specific wave and current information. This investigation is fortunate in that recently obtained current data for several locations near and within the disposal site are available. Current measurements, collected by the National Oceanic and Atmospheric Administration (NOAA) as a component of the Charleston Harbor Oceanography Project, were provided to the Coastal Engineering Research Center (CERC), US Army Engineer Waterways Experiment Station (WES), for analysis and use in this study. One current meter was placed within the limits of the ODMDS by the EPA to provide information on local currents. These data were also supplied to CERC for use in this study.

5. This report concentrates on the three primary components of the study: boundary condition development, short-term modeling, and long-term modeling. The most important component of the three is the development of realistic boundary conditions at the site. The accuracy and credibility of the numerical modeling effort are dependent on the realistic approximation of waves and currents at the disposal site. The importance of this aspect of the study has been stressed in similar site characterization studies and will be the subject of Part II of this report.

PART II: WAVE AND CURRENT BOUNDARY CONDITIONS

6. The short-term modeling phase of this analysis requires the specification of a local velocity field representative of the conditions found at the disposal site. Because the DIFID model applies only to the time immediately following disposal, a single-value velocity is specified to represent a "worst-case dispersion scenario" in which the currents are directed from the disposal site to the live bottom habitat regions. In this manner, a single-value, depth-averaged velocity can be used to quantify the potential effect of the disposal operation on the reefs.

7. The long-term modeling phase requires a more nearly complete and comprehensive description of local waves and currents because the modeling approach investigates the behavior of a disposal mound over long periods of time (on the order of months). As such, a realistic representation of the wave and current time series is required for the site; otherwise realistic predictions of mound stability cannot be made. The remaining paragraphs of Part II will concentrate on defining the wave and current boundary conditions required as input to both the short- and long-term models.

Wave Height, Period, and Direction Time Series

8. The long-term transport model computes sediment transport as a function of time series of both waves and currents. The wave time series component is specified as a statistical simulation of the 20-year hindcast data base of the Wave Information Study (WIS) (Jensen 1983), Phase III, Station 117 "sea" conditions. The location of Station 117 is shown in Figure 2. The statistical approach to defining time series of wave height, period, and direction for a specific WIS station is reported in detail by Borgman and Scheffner (1991). The approach allows the user to simulate wave sequences that preserve the statistical qualities of the entire 20-year data base, including seasonality and wave sequencing. The statistically based time series provides a site specific wave climate that is ideal for the long-term simulation.

9. A 1-year time series of waves was generated as input for the long-term model. Plots of the simulated sequence of wave height, period, and direction are shown in Figure 3. To demonstrate the visual similarity between the simulated wave field and actual hindcast data, Figure 4 represents a

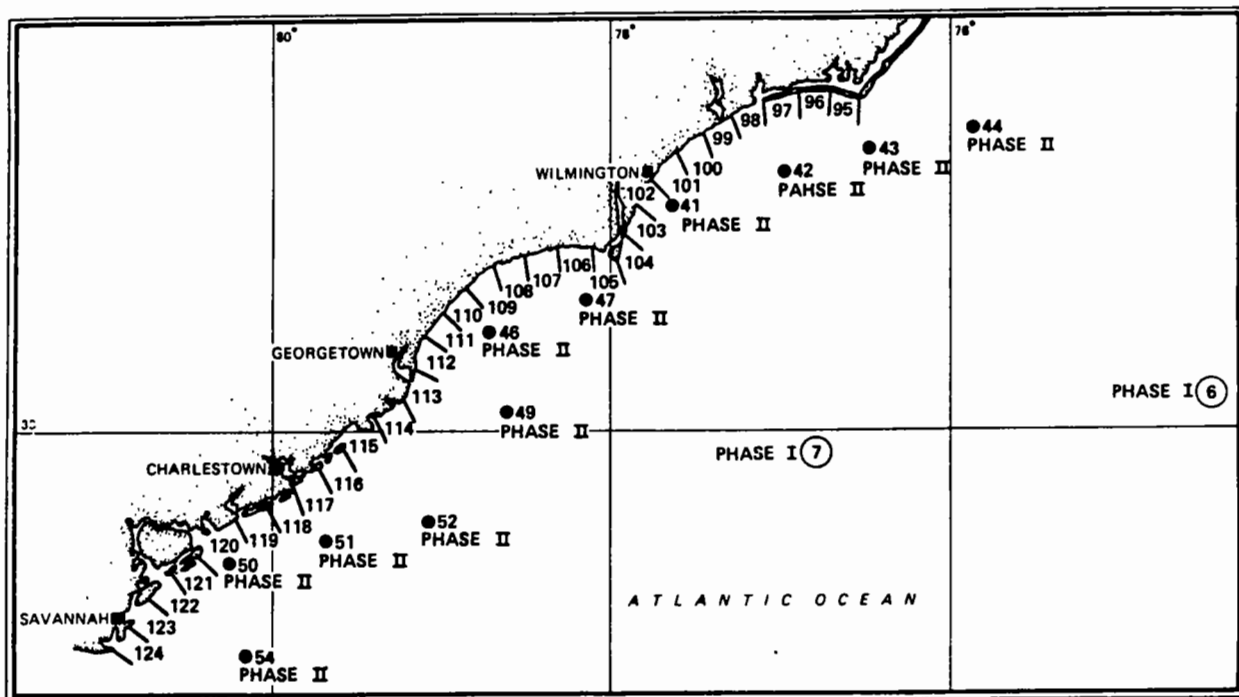
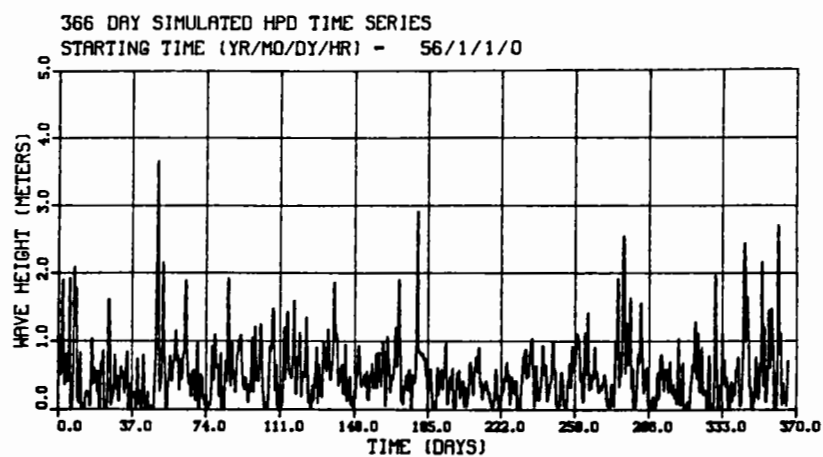
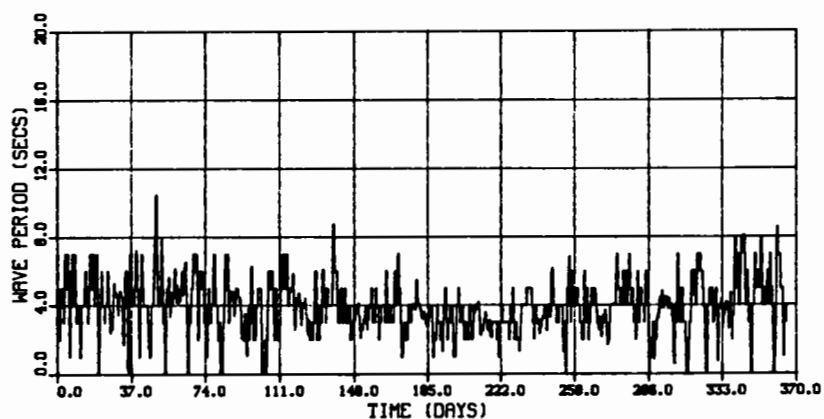


Figure 2. WIS hindcast data station locations

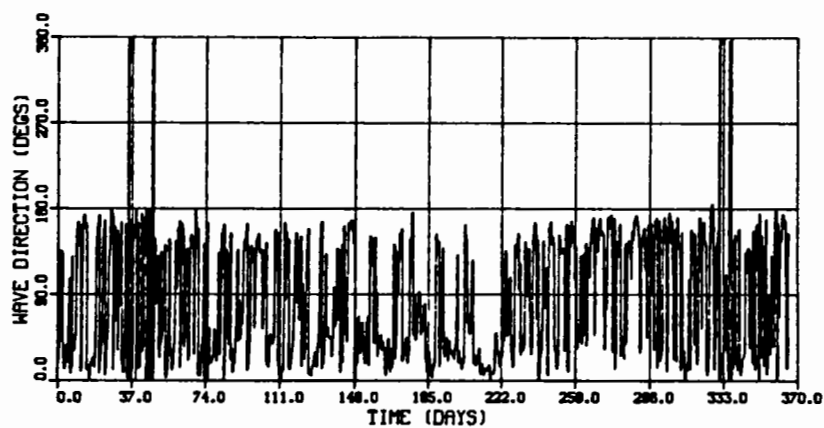
1-year time series of WIS data for the year 1956. Both Figures 3 and 4 begin on 1 January and extend through 31 December. The similarity in patterns of increased winter activity with a decrease in intensity during the summer months can be seen in both plots. A quantitative comparison of the data can be seen in the percent probability histogram plots shown in Figure 5, in which the probability statistics of the simulated wave height, period, and direction are overlaid with those of the 1956 WIS data. A compilation of computed maximum, minimum, average, and standard deviation values for both the simulated data and the hindcast data for the years of 1956, 1960, 1964, and 1968 are shown in Table 1. The similarity in values demonstrates that the simulated time series are statistically similar to the hindcast data base. Also included in Table 1 is the direction from which the greatest number of waves originated. The reported angles are with respect to a shore-parallel baseline so that 90 deg indicates a wave field directed onshore. Computations indicate that the majority of waves are from the northeast and southwest. This observation is consistent with the bimodal directional distribution of the WIS data shown in the directional histogram of Figure 5.



a. Wave height



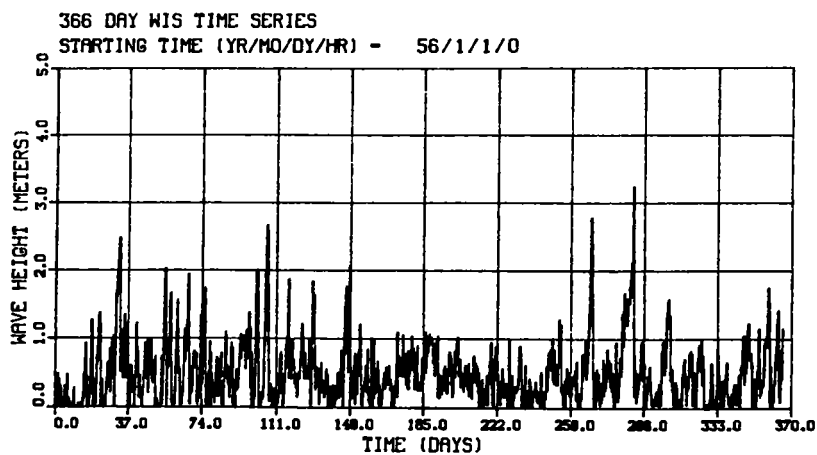
b. Wave period



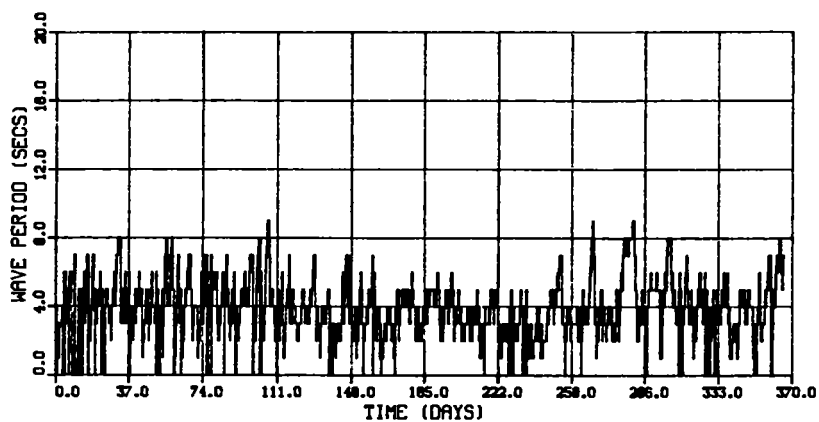
PHASE III STATION 117 - CHARLESTON

c. Wave direction

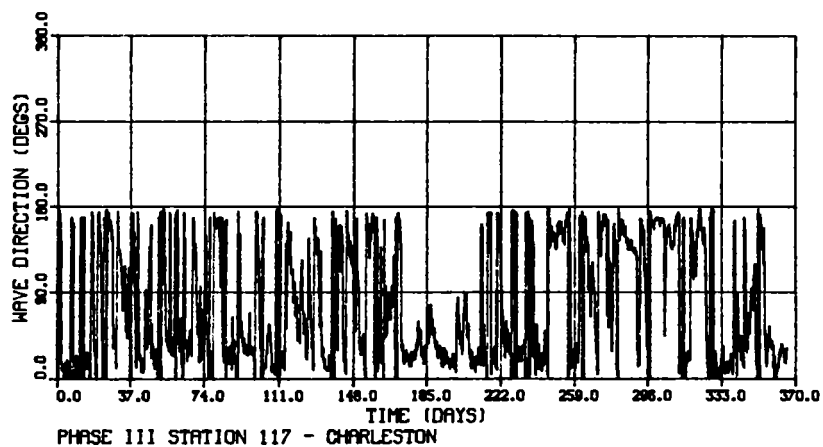
Figure 3. Simulated 1-year time series of wave height, period, and direction



a. Wave height

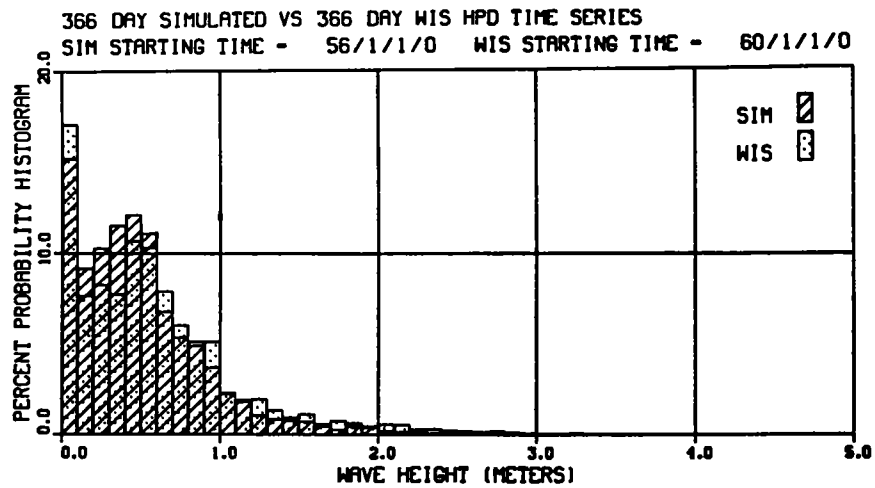


b. Wave period

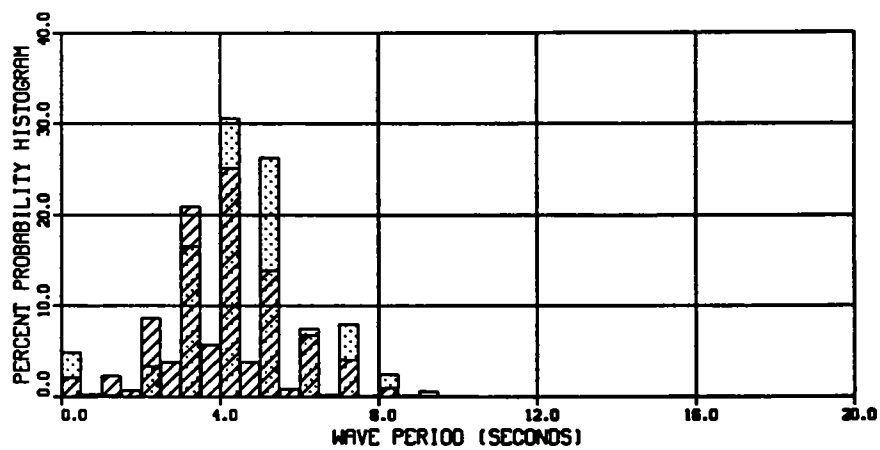


c. Wave direction

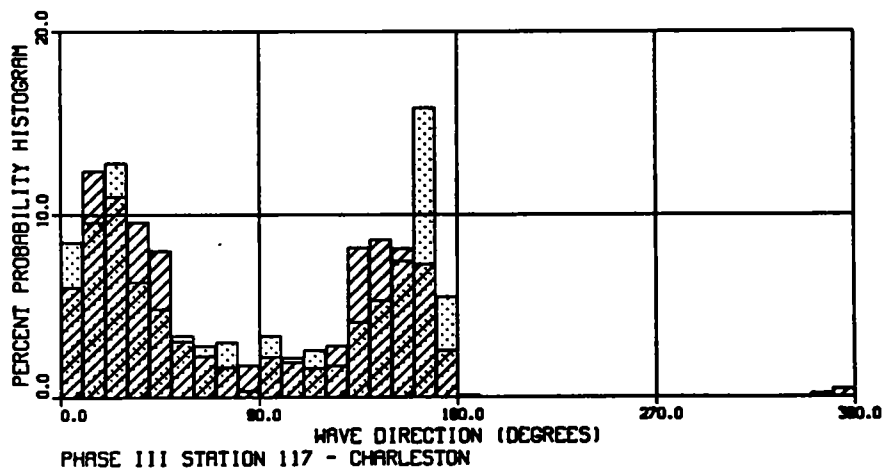
Figure 4. WIS Station 69 Time Series for 1956



a. Wave height



b. Wave period



c. Wave direction

Figure 5. Probability histograms for simulated wave and 1956 WIS data

Table 1
Comparison of Wave Statistics

<u>Parameter</u>	<u>Simulated</u>	<u>1956</u>	<u>1960</u>	<u>1964</u>	<u>1968</u>
Maximum wave height, m	3.7	3.3	3.3	3.3	2.9
Minimum wave height, m	0.0	0.0	0.0	0.0	0.0
Average wave height, m	0.5	0.5	0.6	0.6	0.3
Standard deviation, m	0.4	0.4	0.5	0.6	0.4
Maximum wave period, sec	10.5	9.0	9.0	9.0	9.0
Minimum wave period, sec	0.0	0.0	0.0	0.0	0.0
Average wave period, sec	3.9	3.8	4.4	4.4	2.9
Standard deviation, sec	1.5	1.8	1.7	1.7	1.9
Most common direction, deg	10-20	20-30	160-170	160-170	0-10

10. Station 117 represents a Phase III WIS hindcast station, and as such, the hindcast is developed for 10 m of water. The following relationships were used to transform the wave height from 10 m to deep water and then to shoal the wave from deep water back to the disposal site. This transformation maintains the proper wave height relationship for the wave shoaling in response to the presence of the disposal site (Ebersole, Cialone, and Prater 1986):

$$H = H_0 k_s \quad (1)$$

where the shoaling coefficient k_s is defined as:

$$k_s = \left\{ \frac{1}{\left[1 + \frac{2kh}{\sinh(2kh)} \right] \tanh(kh)} \right\}^{1/2} \quad (2)$$

The parameters k and h represent the wave number and local depth, respectively.

Depth-Averaged Current Time Series

11. The analysis of the velocity patterns in the vicinity of the ODMDS begins with an analysis of the multiple-depth NOAA data, since that data

provides information on current variations with respect to depth. Results will then be supplemented and enhanced by the single-gage EPA data located 6 ft off the bottom within the boundaries of the disposal site.

12. The current information was recorded with bottom-moored, self-contained, acoustic doppler profilers manufactured by RDI Instruments Inc. Data were provided for the four locations shown in Figure 6. Summary statistics of each instrument location are given in Table 2.

13. Since depth-averaged currents are used for the present analysis, a depth-averaged value at each time-step was computed by averaging the values for the depth through the water column at each 10-sec time-step of the time series shown in Table 2. A six-constituent harmonic analysis was performed on the depth-averaged data to provide an indication of tidal influence in the tidal signal. Results of the analysis are summarized in Table 3. The reported reduction in variance (RV) values indicates the degree of tidal

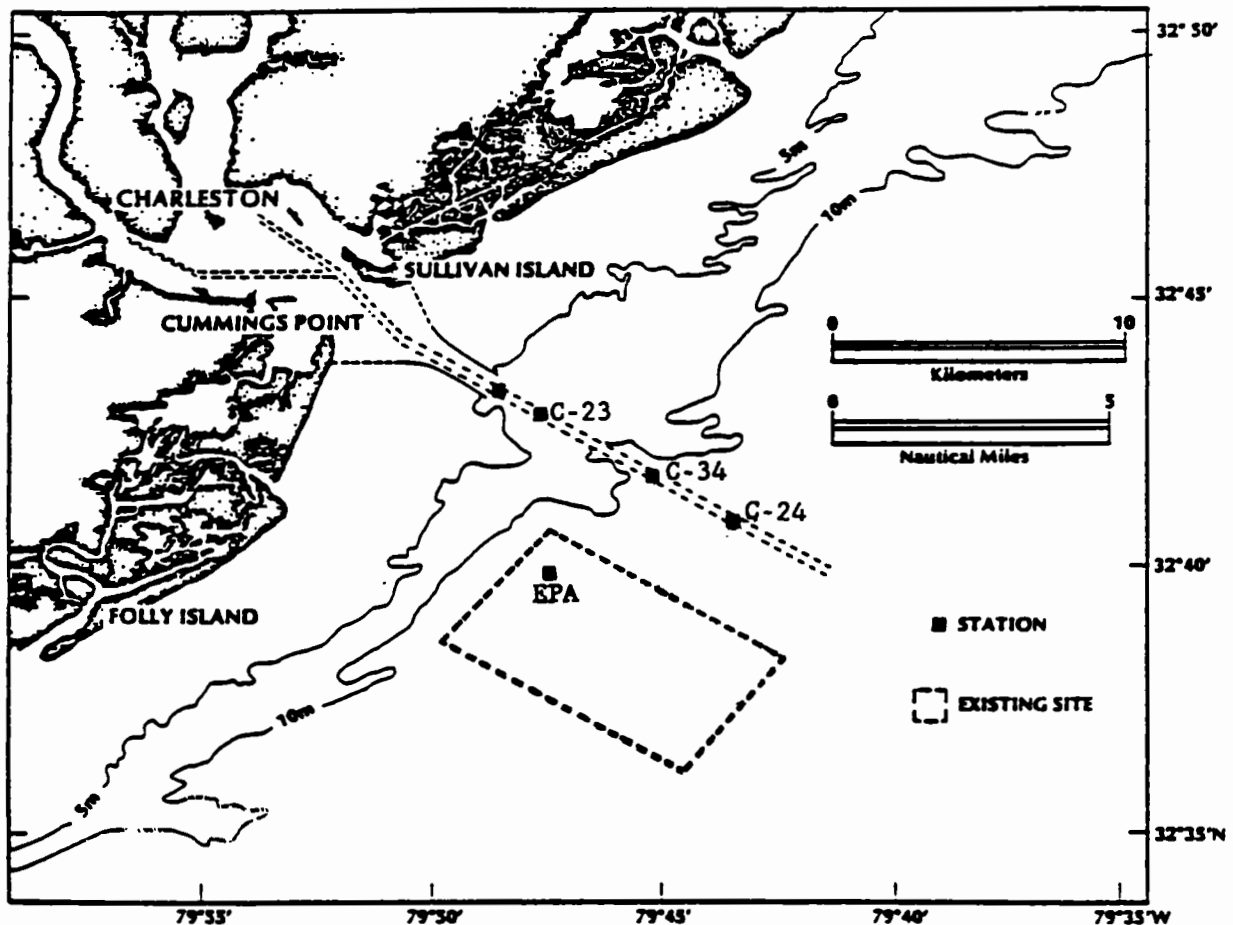


Figure 6. Station locations for current meter data

Table 2
Summary Statistics of NOAA Current Data

Depth m	Mean Velocity		Standard Deviation	
	cm/sec		cm/sec	
	U	V	U	V
<u>Station C-23</u>				
<u>Location (lat/long): 79.7923/32.7150</u>				
<u>Sampling period: 17 May 1988 - 21 June 1988</u>				
0.9	18.7	-6.1	30.3	22.1
1.9	17.0	-6.0	29.1	21.6
3.0	13.7	-4.1	26.8	19.8
4.1	10.7	-3.0	24.8	18.7
5.2	7.9	-2.3	22.8	18.0
6.3	5.0	-1.8	20.9	17.4
7.4	2.2	-1.5	19.3	16.7
8.4	-0.4	-1.2	18.0	15.8

<u>Station C-24</u>				
<u>Location (lat/long): 79.7260/32.6830</u>				
<u>Sampling period: 17 May 1988 - 21 June 1988</u>				
0.3	7.9	2.4	23.	18.2
1.3	6.0	2.6	18.	12.8
2.3	6.9	2.3	19.	12.8
3.3	6.1	2.3	18.	12.7
4.3	4.9	2.3	17.	12.3
5.3	3.5	2.5	16.	12.0
6.3	2.2	2.8	14.	11.5
7.3	1.1	3.0	13.	11.5
8.3	0.3	3.0	12.	10.2
9.3	0.8	3.0	12.	9.9

<u>Station C-33</u>				
<u>Location (lat/long): 79.8100/32.7243</u>				
<u>Sampling Period: 21 June 1989 - 18 Sep 1989</u>				
0.0	23.0	-5.9	50.	37.1
1.1	17.5	-7.0	48.	29.1
2.2	15.3	10.9	49.	29.1
3.3	11.6	11.4	48.	28.0
4.4	7.5	-9.8	46.	26.5
5.5	3.5	-9.5	44.	24.7
6.6	0.1	-9.5	41.	22.8
7.7	-2.1	-9.9	38.	20.6

(Continued)

Note: Station locations indicated by latitude and longitude.

Table 2 (Concluded)

Depth m	Mean Velocity		Standard Deviation	
	cm/sec		cm/sec	
	U	V	U	V
<u>Station C-34</u>				
<u>Location (lat/long): 79.7557/32.6947</u>				
<u>Sampling Period: 21 June 1989 - 18 Sep 1989</u>				
0.0	4.0	1.4	19.	14.1
1.0	6.8	1.6	19.	14.1
2.0	8.0	1.4	19.	13.3
3.0	6.8	1.4	19.	12.4
4.0	6.6	1.3	20.	13.0
5.0	5.4	2.0	19.	13.2
6.0	3.8	2.7	18.	12.8
7.0	2.8	3.2	17.	12.6
8.0	1.3	3.7	16.	12.1
9.0	0.7	3.7	14.	11.3
0.0	1.2	3.4	14.	10.5

Table 3

Harmonic Analysis Summary

Const.*	C-23		C-24		C-33		C-34	
	U	V	U	V	U	V	U	V
M ₂	26.17	20.27	16.31	7.24	57.82	29.59	18.54	9.41
S ₂	3.73	3.15	1.77	2.36	7.73	4.11	2.37	1.41
N ₂	5.09	4.51	1.01	1.72	9.97	3.52	3.22	1.76
K ₁	3.70	0.42	0.88	2.15	5.95	3.34	1.88	0.24
O ₁	5.11	2.47	2.05	1.31	4.06	2.00	1.34	0.50
P ₁	8.72	4.29	3.10	1.92	2.18	0.85	1.40	0.10
RV	0.72	0.73	0.5	0.25	0.9	0.71	0.64	0.35
Ave.	9.34	-3.24	3.89	2.61	9.54	9.12	4.30	2.33

* Const. - constituent
ave. - average

influence, a value of 1.0 indicating that the selected six constituents completely describe the time series. Conversely, a value of 0.0 indicates that the time series is uncorrelated with tides. As indicated, the signals are tide dominated and are primarily semidiurnal in period.

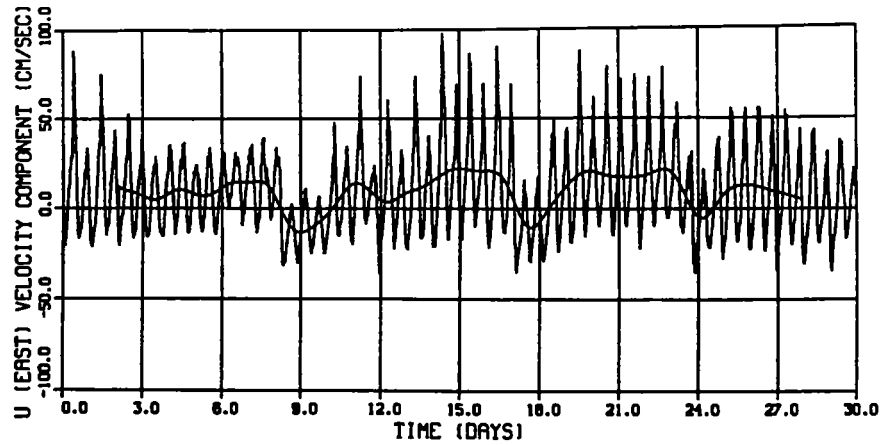
14. A visual indication of the nontidal component of the signal can be demonstrated through the application of a low-pass nonrecursive digital filter that separates the high-frequency (tidal) component of the series from the low-frequency (storm or large-scale circulation) component. Figures 7 through 10 present these data in the form of raw time series and the U (east) and V (north) component with the superimposed low-frequency component. A current direction histogram is also shown.

15. Since the directional histogram provides no information on magnitudes, the direction vector of each U,V pair was computed to indicate the coupling of magnitude and directionality. These relationships are shown in the form of continuous vector plots of each time series (at a 60-min interval) and are illustrated in Figure 11.

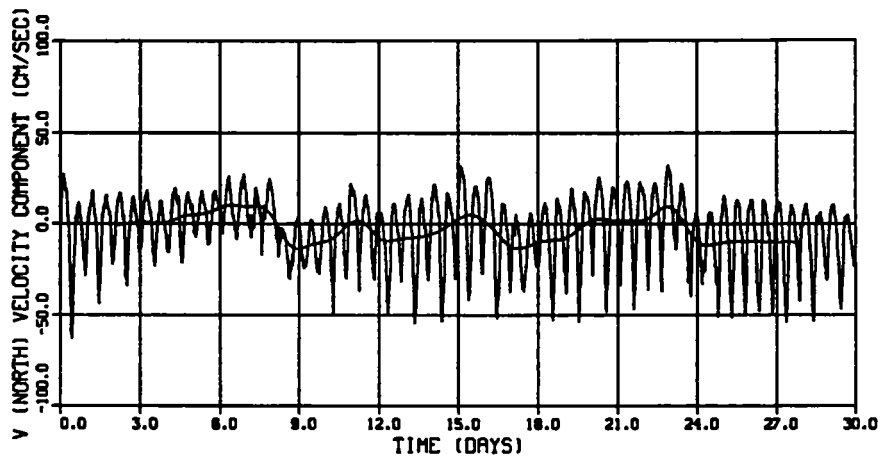
16. An examination of the data from Stations C-23 and (especially) C-34 shows that these current station locations are dominated by the effects of the jetty entrance and therefore are not representative of the currents descriptive of the ODMDS. For example, Station C-33 shows the strong ebb-flow jet directed at an angle of approximately 110 to 130 deg. The flood flow is also shown in the plot; however, the direction varies somewhat around the entrance of the jetty. Data from both Stations C-24 and C-34 are free of the localized effects of the jetty. Both vector plots indicate a tidal ellipse with the major axis oriented to the northeast-southwest and the minor axis approximately 90 deg offset. Since these two gage locations can be considered to be representative of the ODMDS, the uniformity of the currents with respect to depth is investigated to show that the use of a depth-averaged velocity in the numerical modeling effort is justified. Vector plots of each of the time series for each of the depths indicated in Table 2 for Station C-24 are given in Figure 12. Results show similar trends at each depth with an increase in velocity from the bottom to the top.

17. Results of the harmonic analyses as well as the continuous vector diagrams indicate that a velocity field with the characteristics of those shown for gages at Stations C-24 or C-34, i.e. maximum velocity magnitudes on the order of 40 to 50 cm/sec, is representative of current patterns immediately north of the ODMDS. In both cases, residual currents are directed to

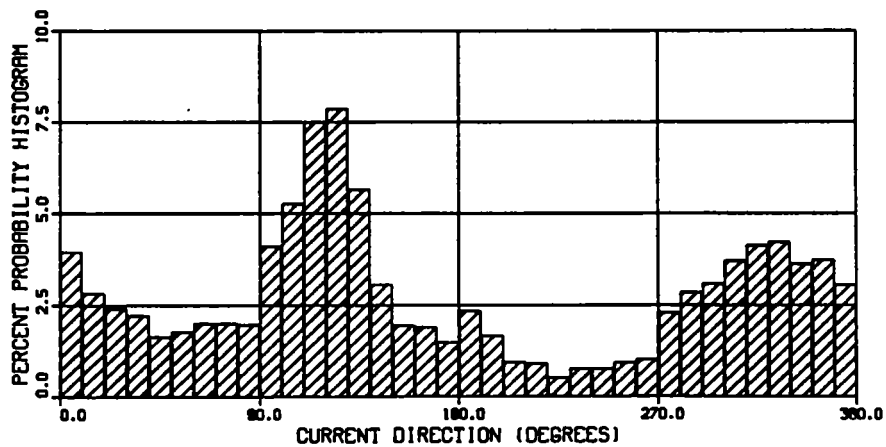
STATION C-23 (DEPTH



a. U component

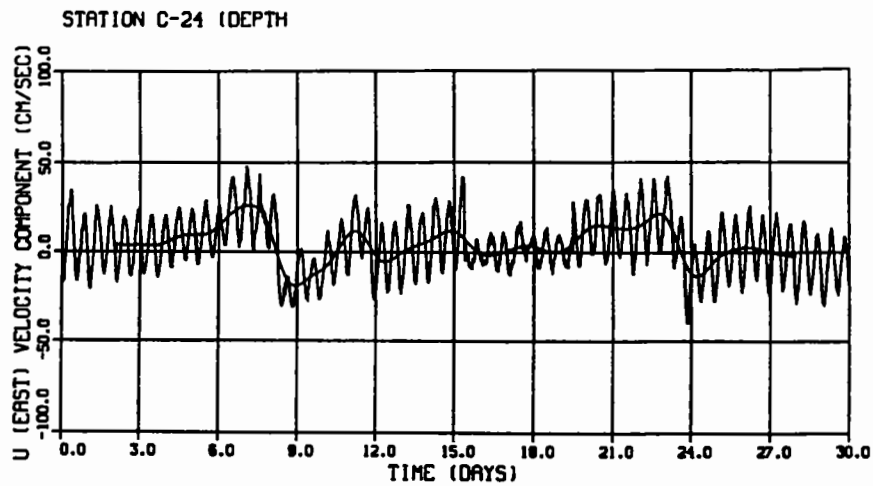


b. V component

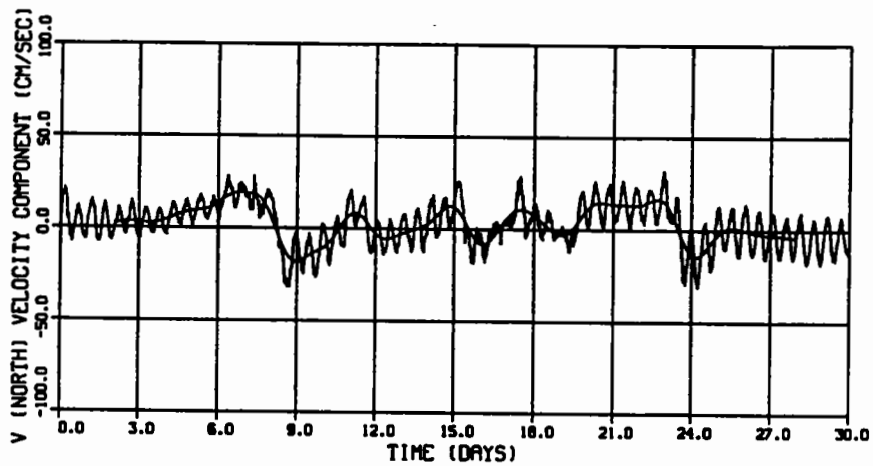


c. Percent probability

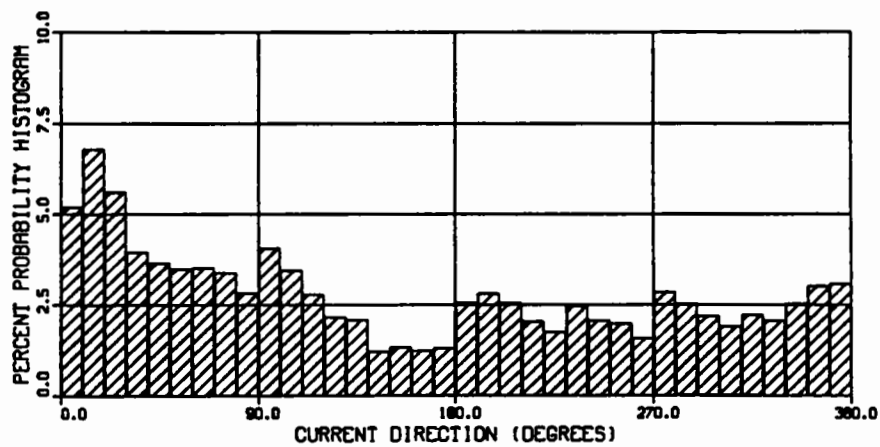
Figure 7. Station C-23 velocity component/directional data



a. U component

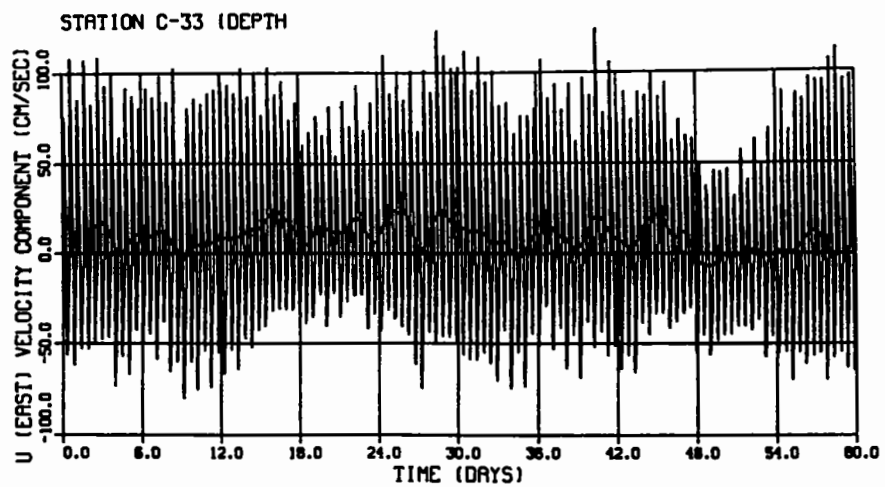


b. V component

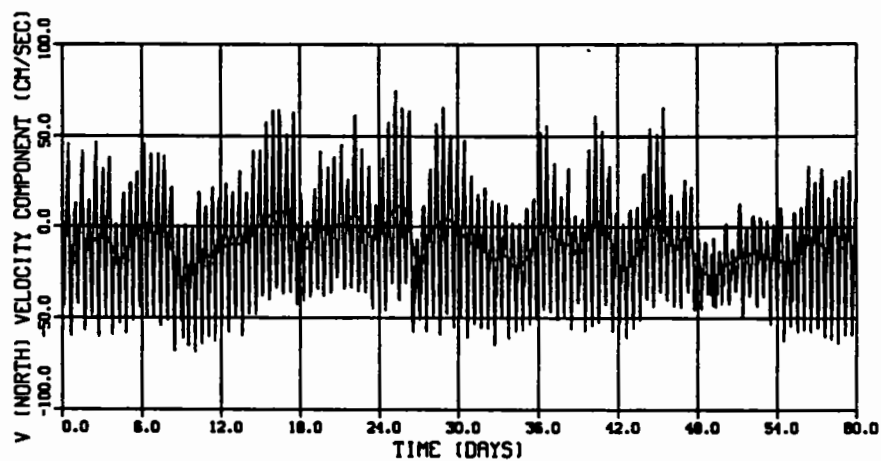


c. Percent probability

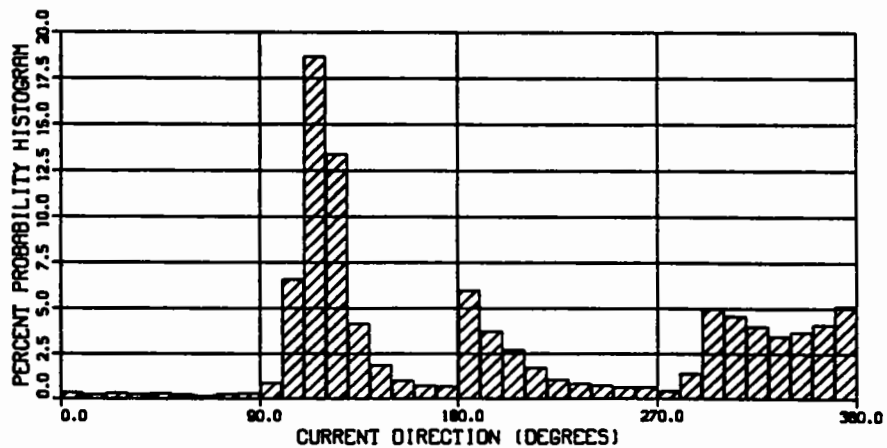
Figure 8. Station C-24 velocity component/directional data



a. U component

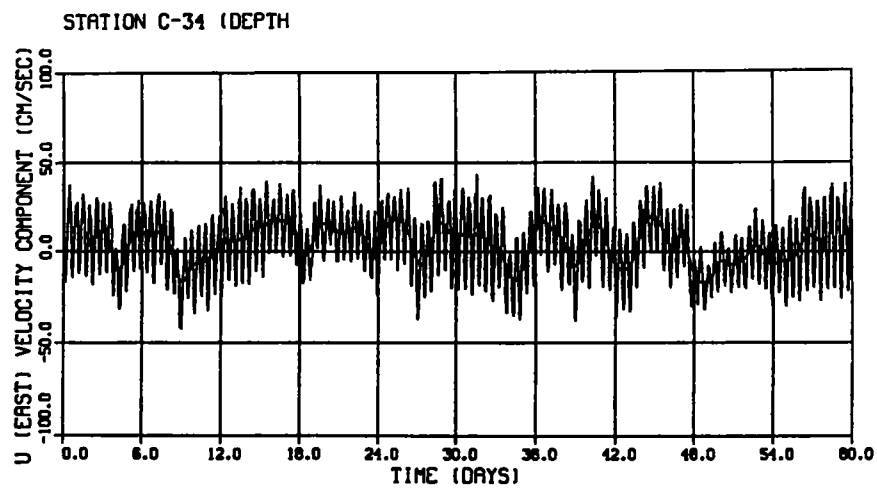


b. V component

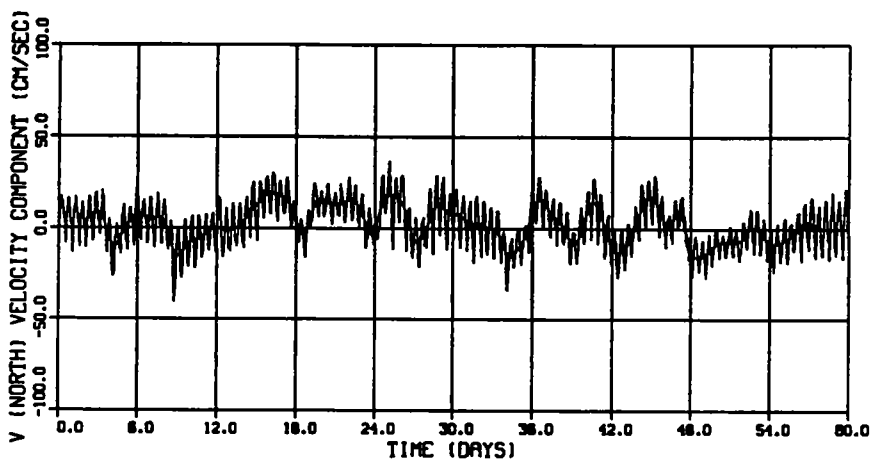


c. Percent probability

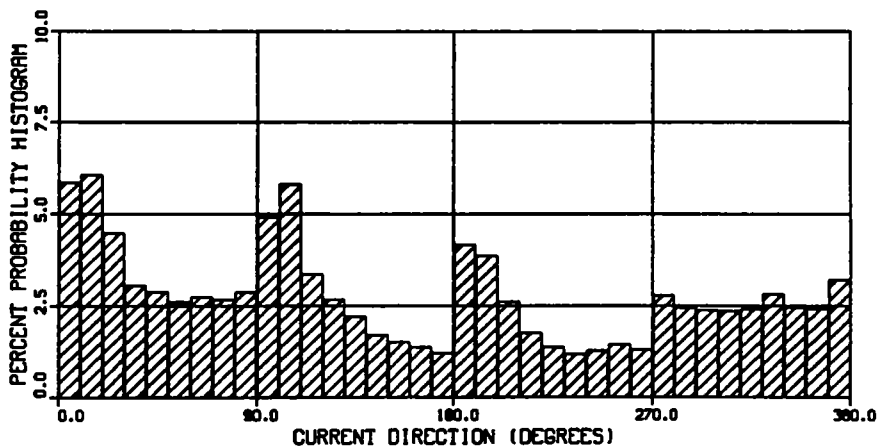
Figure 9. Station C-33 velocity component/directional data



a. U component

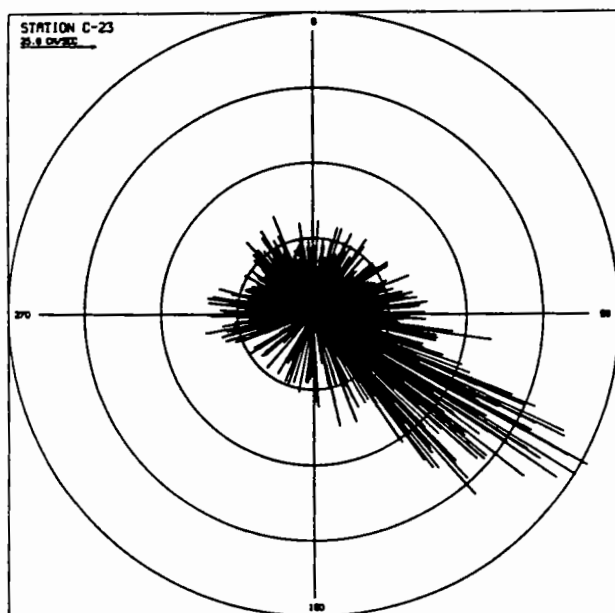


b. V component

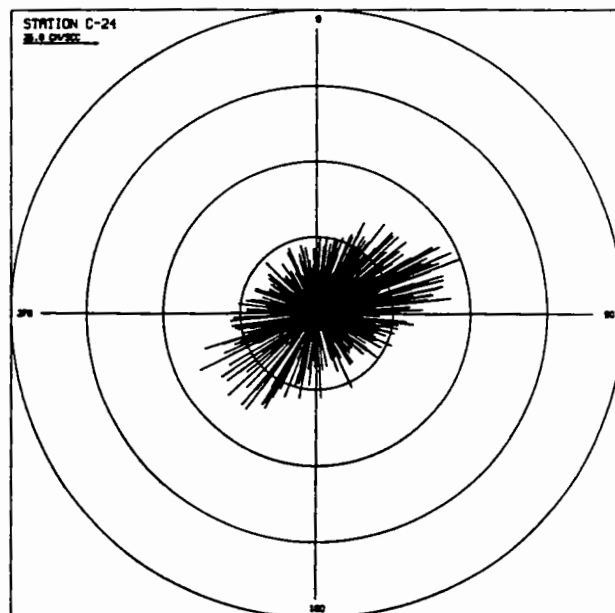


c. Percent probability

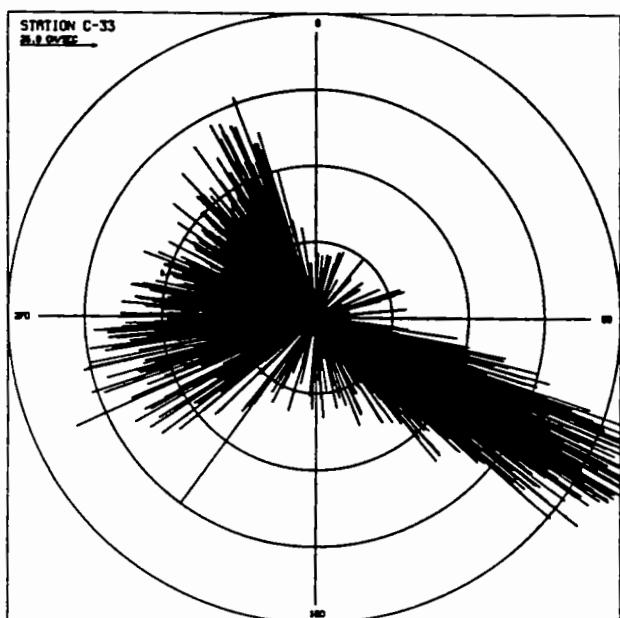
Figure 10. Station C-34 velocity component/directional data



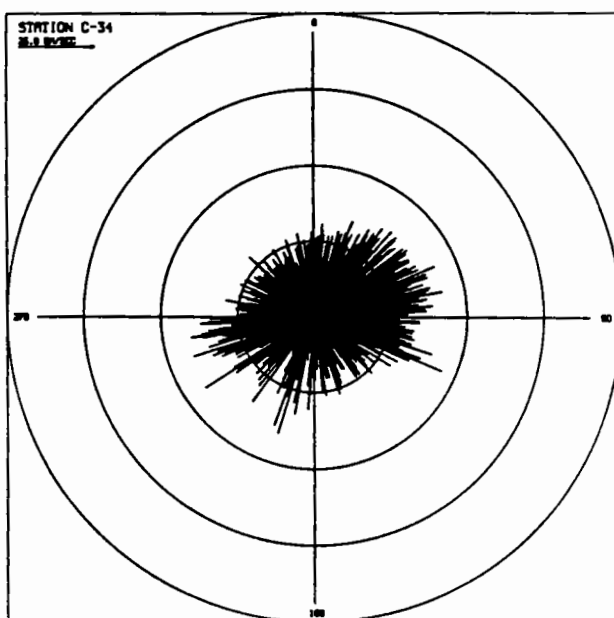
a. C-23



b. C-24

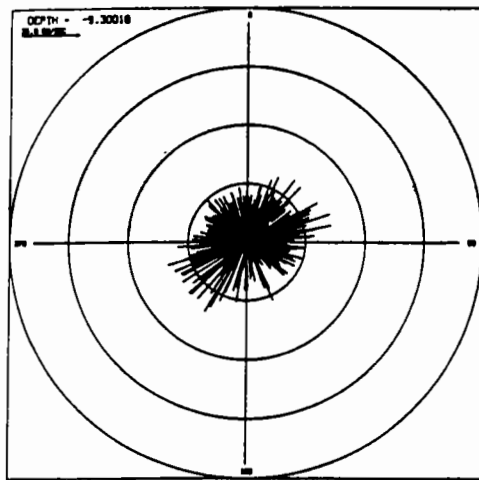


c. C-33

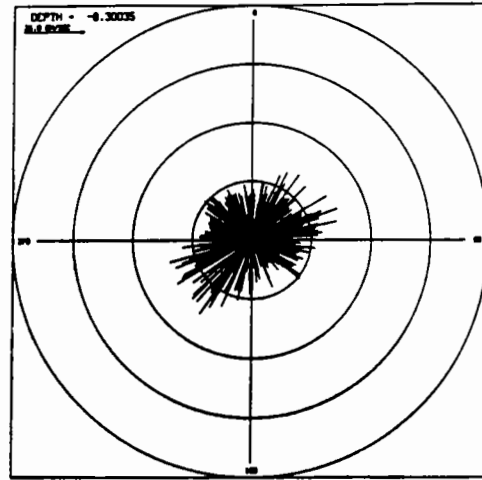


d. C-34

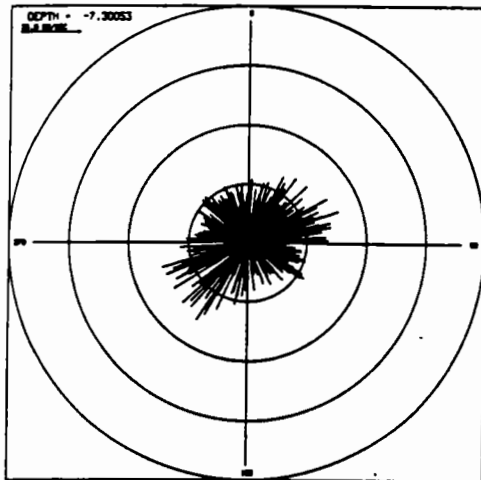
Figure 11. Current vector diagrams



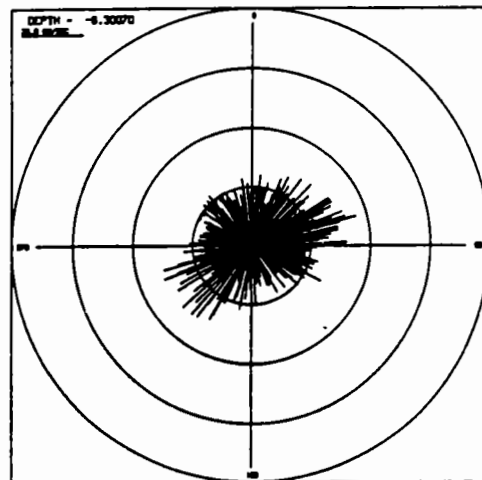
a. 9.30 m



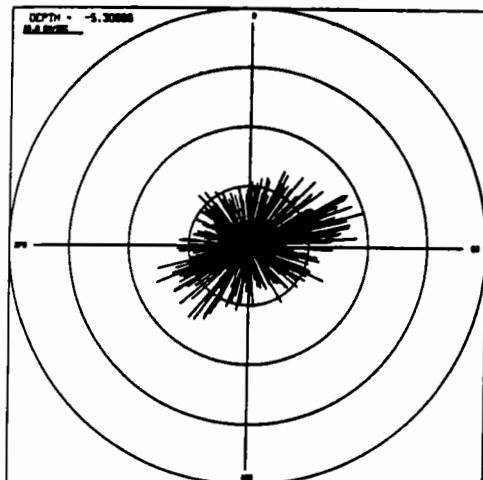
b. 8.30 m



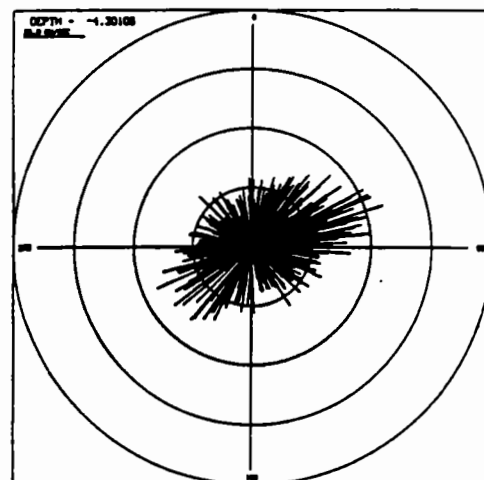
c. 7.30 m



d. 6.30 m

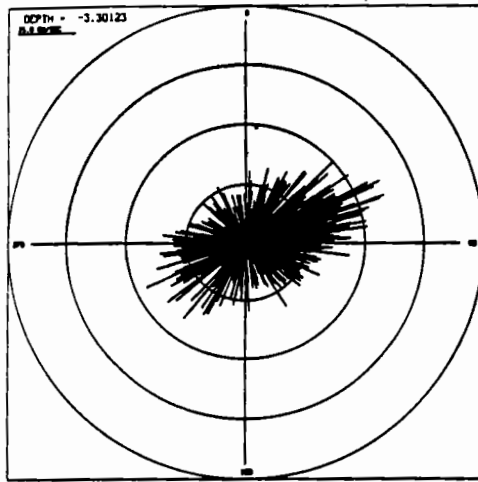


e. 5.30 m

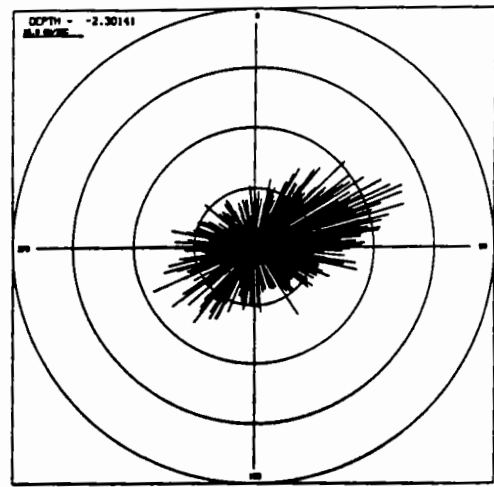


f. 4.30 m

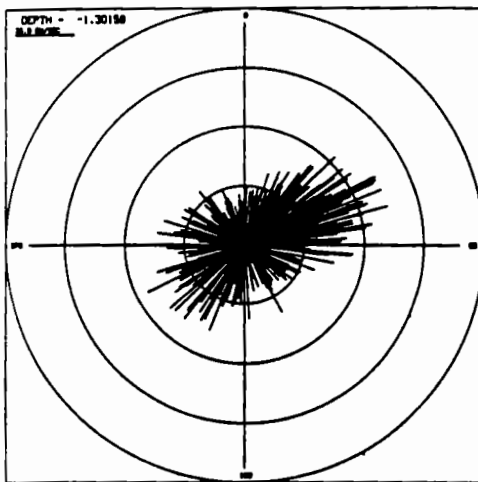
Figure 12. Current vector relationships at Station C-24 (Continued)



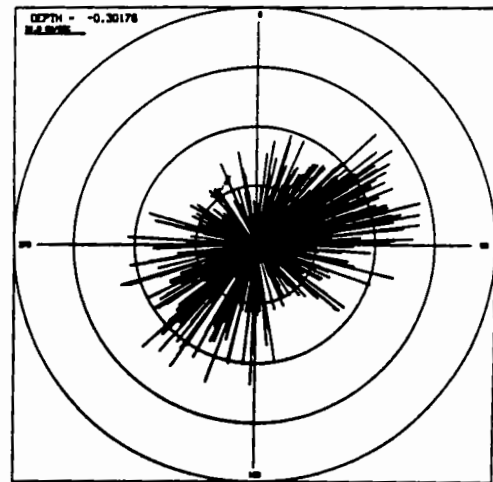
g. 3.30 m



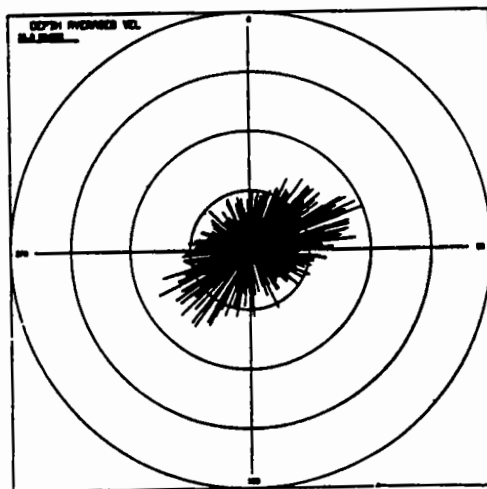
h. 2.30 m



i. 1.30 m



j. 0.30 m



k. Depth averaged

Figure 12. (Concluded)

the northeast. Analysis of the onsite near-bottom mounted EPA gage determined whether currents within the ODMDS are significantly different from those at NOAA sites C-24 and C-34.

18. The EPA current gage is located in the northernmost corner of the ODMDS, as shown in Figure 6. The instrument, an ENDECO Type 174SSM solid state current meter, is located approximately 6 ft from the bottom.* Data were collected during the periods of 21 June-17 July, 24 July-20 Aug, and 15 Nov-11 Dec 1990. Current values with the superimposed low-frequency component and the directional histograms are shown in Figures 13, 14, and 15. Continuous vector plots are shown in Figure 16. Results of the harmonic analyses of the three data series are presented in Table 4.

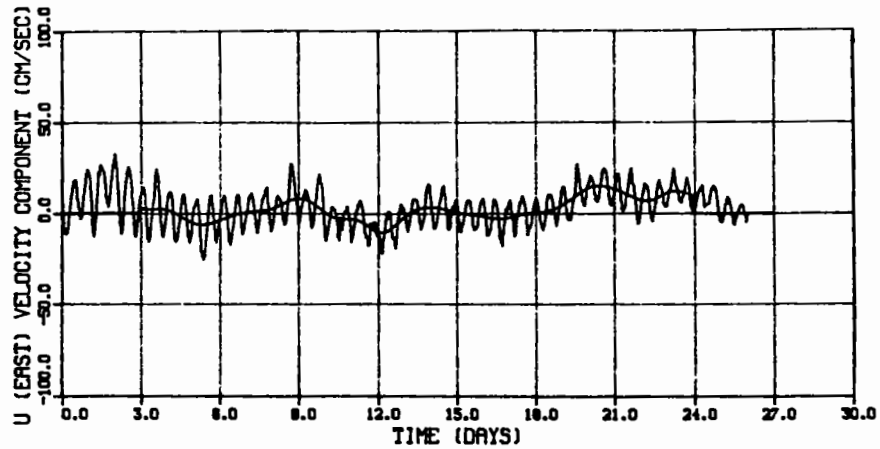
19. Analysis of the data presented in Table 4 and Figures 13 through 16 indicates that currents at the EPA gage site are similar in both magnitude and orientation to those of NOAA Stations C-24 and C-34. For example, the combined series vector plot shown in Figure 16 is similar in qualitative details to the near-bottom vector plots for NOAA Station C-24, shown in Figures 12a and b. It is therefore reasonable to assume that the depth-averaged harmonic constituents computed for Station C-24 can be used to characterize the tidal forcing at the Charleston ODMDS.

20. The harmonic analyses indicate that approximately 50 to 60 percent of the currents can be attributed to tides. To account for the source of the variance, a low-frequency component, similar in magnitude to those shown in Figures 8, 10, and 12 through 14, is introduced to simulate the low-frequency component of the observed time series.

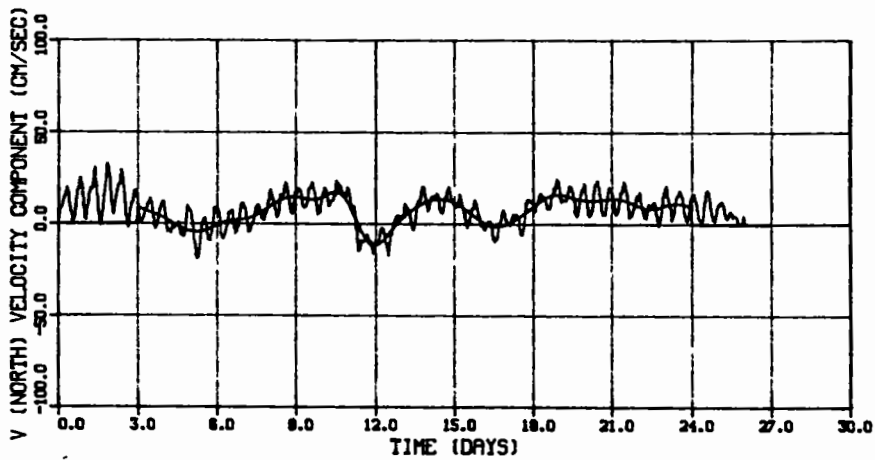
21. The long-term modeling goal is to generate a data base of simulated current data that is realistically representative of currents at the disposal site. In the same manner that the wave fields were simulated to reflect the observed statistical distribution of the WIS hindcast data, a time series of currents was prepared for the ODMDS, based on the harmonic constituents for NOAA Station C-24, shown in Table 3. Although the data are not of sufficient length for a reliable harmonic analysis, the procedure provides an approximate estimate of tidal influence. Inspection of the low- and high-frequency portions of the velocity magnitude as well as the actual U and V components of the data shown in Figures 8 and 10 suggest that the addition of a long-period,

* Personal Communication, Dec 1990, Philip Murphey, Physical Scientist, Environmental Protection Agency.

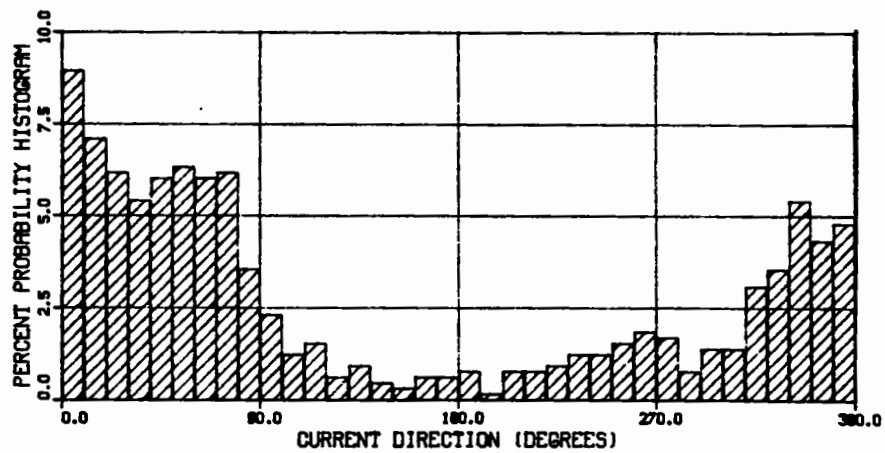
21 JUN - 17 JUL 1990



a. U component



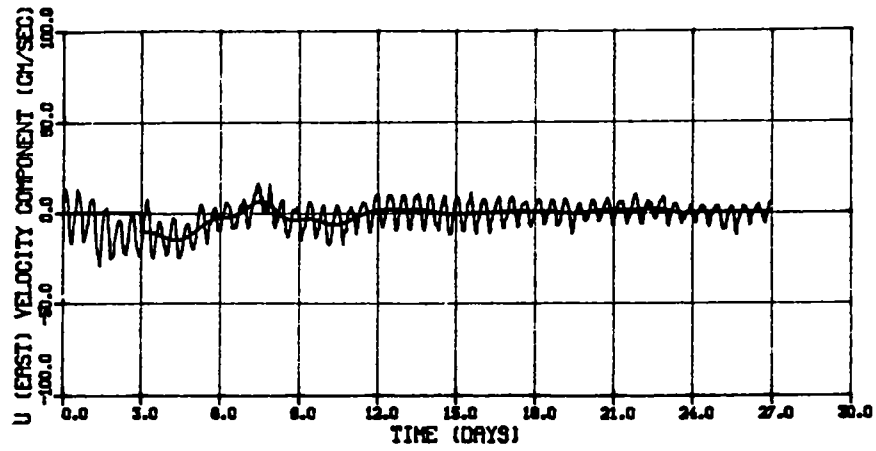
b. V component



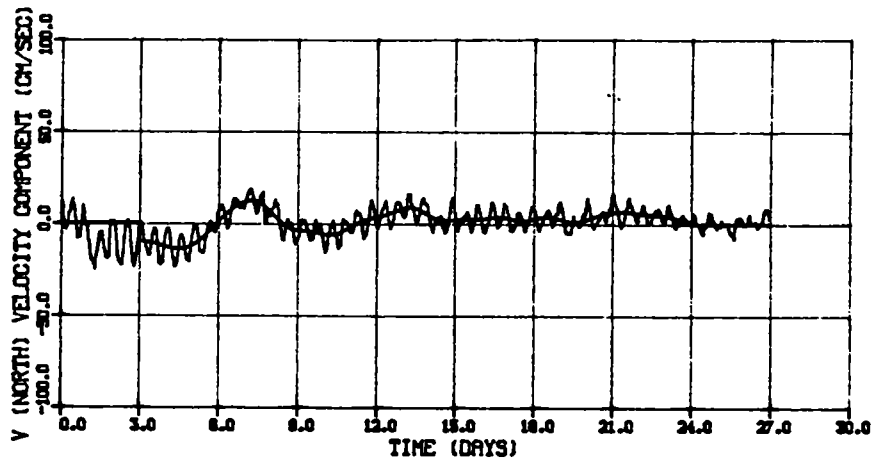
c. Percent probability

Figure 13. Series 1 velocity component/directional data

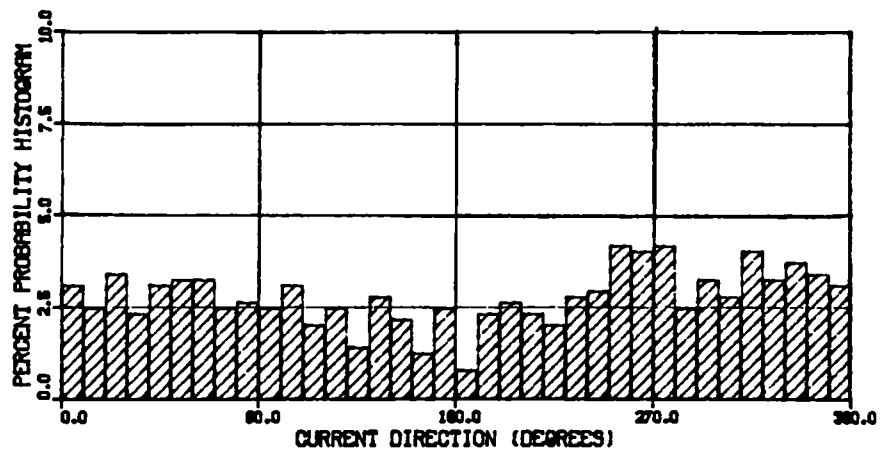
24 JUL - 20 AUG 1980



a. U component



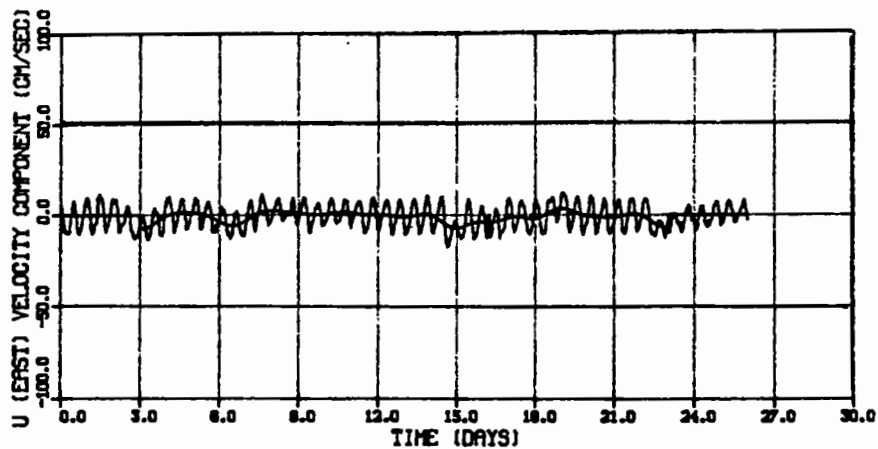
b. V component



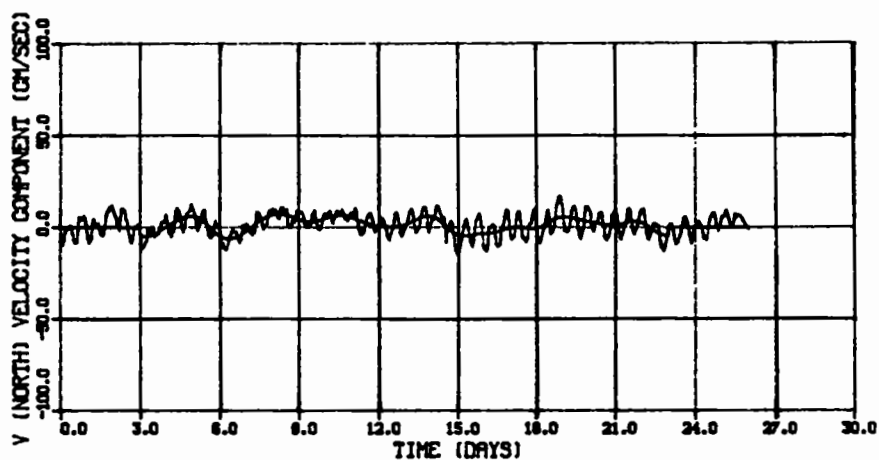
c. Percent probability

Figure 14. Series 2 velocity component/directional data

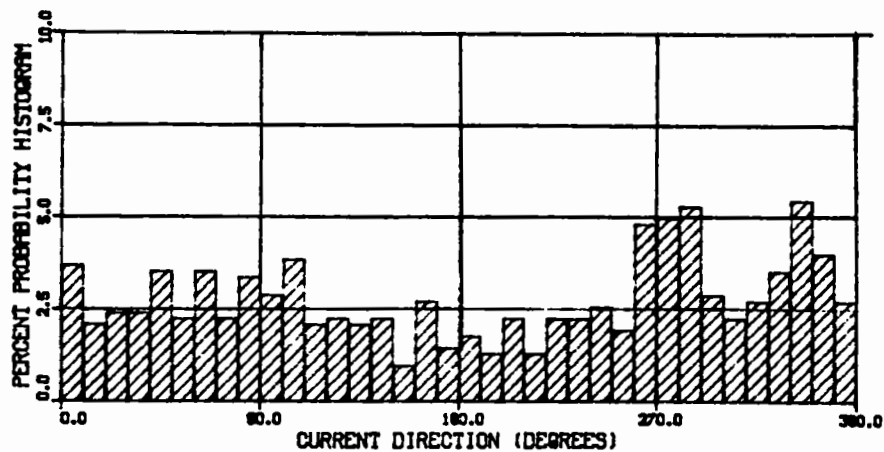
15 NOV - 11 DEC 1990



a. U component

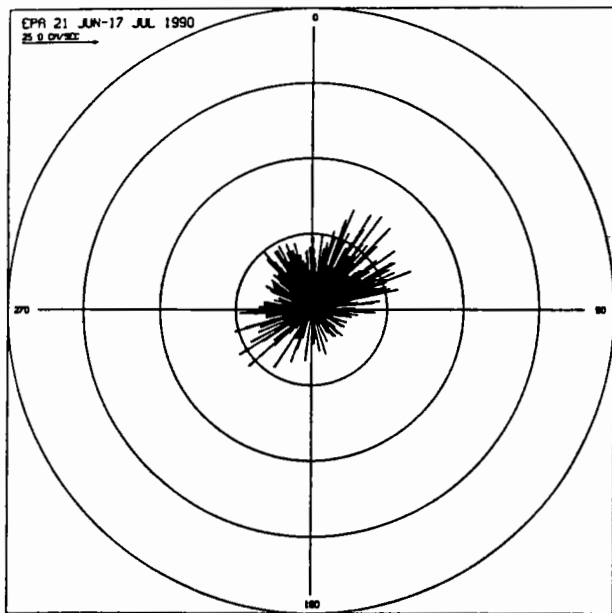


b. V component

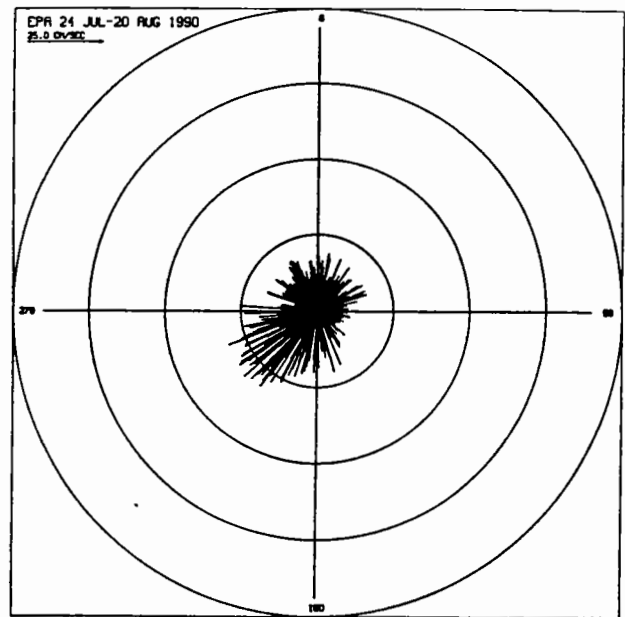


c. Percent probability

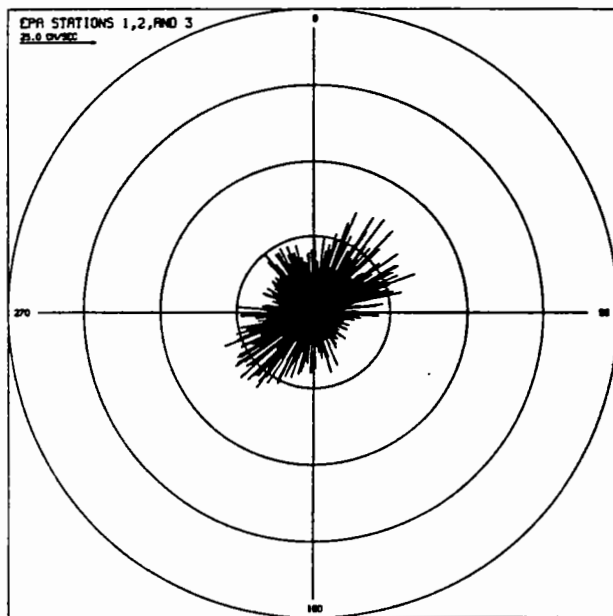
Figure 15. Series 3 velocity component/directional data



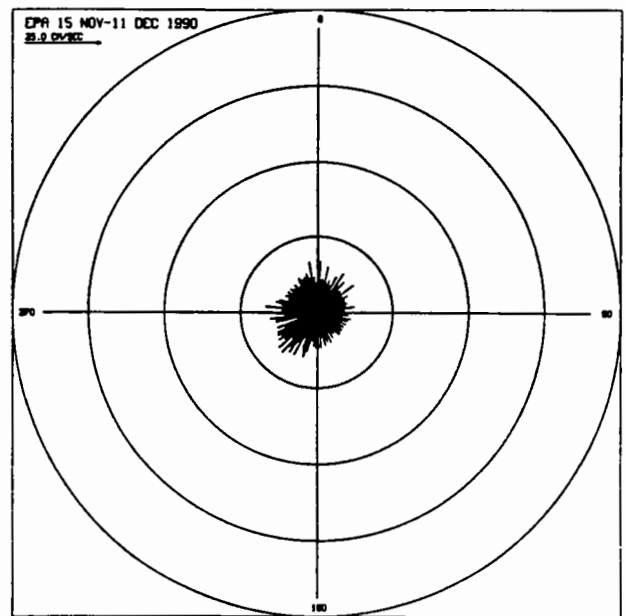
a. Series 1



b. Series 2



c. Series 3



d. Series 1,2, and 3

Figure 16. Current vector diagrams

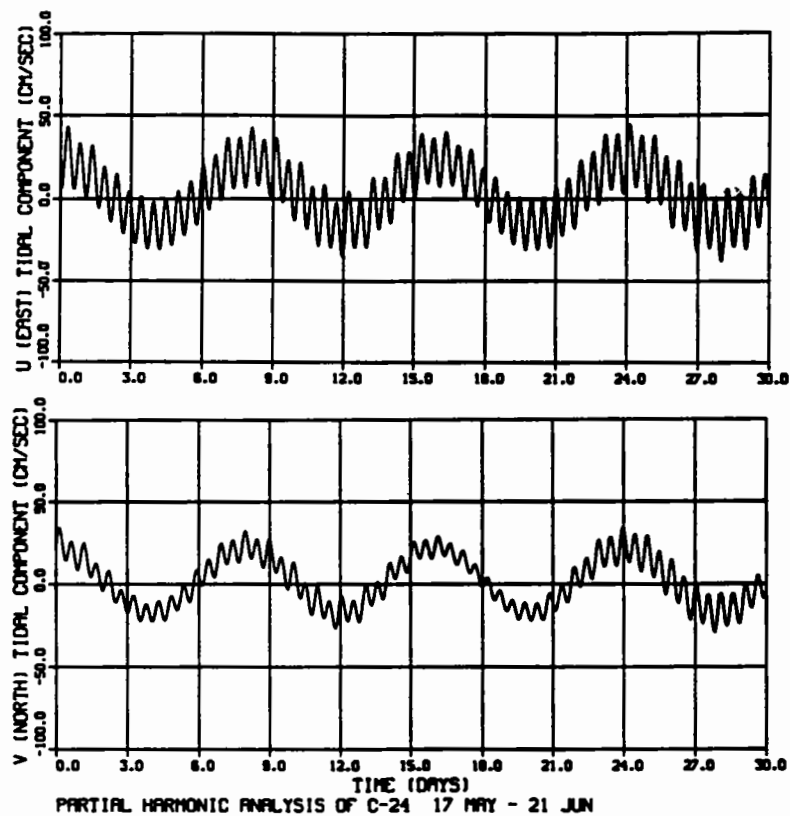
Table 4
Harmonic Analysis Summary, EPA Data

Const.*	Series #1		Series #2		Series #3	
	21 June - 17 July		24 July - 20 Aug		15 Nov - 11 Dec	
	U	V	U	V	U	V
M ₂	10.40	6.25	7.88	5.44	7.41	5.21
S ₂	1.19	0.90	1.43	0.67	0.77	1.26
N ₂	2.70	1.94	1.44	1.15	1.69	2.04
K ₁	5.22	1.87	1.44	3.24	0.38	0.44
O ₁	0.63	0.61	0.61	0.83	0.07	0.56
P ₁	4.17	3.26	1.31	2.23	0.17	0.50
RV	0.55	0.30	0.50	0.26	0.68	0.48
Ave.	3.21	7.75	-2.10	0.33	-1.11	1.29

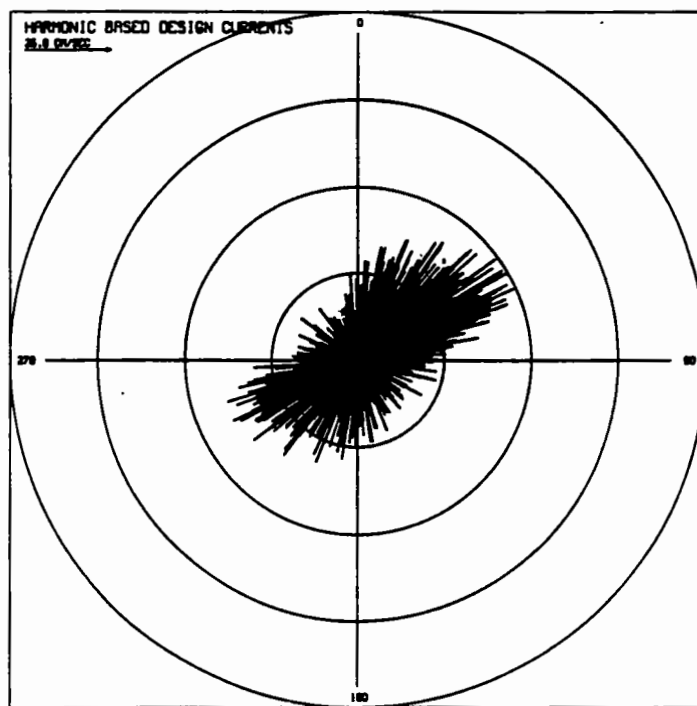
* Const. = constituent
 Ave. = average

large-amplitude component to the tidal signal would produce fluctuations in the simulated current time series that would be representative of prototype conditions. Therefore, a synthetic U and V tidal component with an amplitude of 20 cm/sec and a period of 8 days was added to the constituent list shown in Table 3. The resulting tidal signal and vector is shown in Figure 17. Note that the magnitude envelopes are similar in structure to the observed prototype data. Therefore, the tidal constituents listed in Table 3 and the 8-day low-frequency component are used to simulate tidal height and current fluctuation in the long-term modeling effort. A residual current of U = 3.9 and V = 2.6 cm/sec was included in the synthesized tidal signal (values calculated for C-24).

22. A single-value velocity is specified for the short-term modeling effort since the model simulations correspond only to a single disposal. To represent "worst-case scenarios," maximum envelope current values were selected to simulate the maximum spatial excursion of suspended sediment following release from the barge. In view of the magnitudes shown in Figure 11, two depth-averaged current values were specified for the short-term simulations. A value of 45.7 cm/sec was specified for the northeast-southwest oriented major axis, and a value of 30.5 cm/sec was specified for the northwest-southeast oriented minor axis of the current ellipse.



a. Tidal signal plots



b. Vector plot

Figure 17. Simulated current time-series and vector diagram

PART III: SHORT-TERM MODELING

General

23. The short-term modeling component of this investigation examines the immediate effect of the actual disposal operation on the surrounding area. Numerical simulations of the discharge are used to determine whether the combined effects of the local topography at the site and the depth-averaged velocity field pose a threat to the effectiveness of the dredged material disposal operation. Can the material be physically placed within the limits of the designated site as the material descends through the water column to the ocean floor, or are the local currents of sufficient magnitude to transport material out of the site before deposition?

24. The short-term site evaluation phase is made by numerically modeling the disposal operation using the DIFID numerical model. Theory and background of the model are reported by Johnson and Holiday (1978), Johnson (1990), and Johnson, Trawle, and Adamec (1988). Applications of the model are reported by Trawle and Johnson (1986), Scheffner (1992 and in preparation), and Scheffner and Swain (in preparation). The model computes the time history of a single disposal operation from the time the dredged material is released from the barge until it reaches equilibrium on the ocean floor. The DIFID model separates the dumping operation into three distinct phases. In the first phase, material released from the bin is assumed to form a hemispherically shaped cloud, which descends through the water column under the influence of gravity. This phase is called the convective descent phase.

25. The convective descent phase continues until the cloud of material impacts the bottom or reaches a stable point of neutral buoyancy. In either case, horizontal spreading of material marks the beginning of the dynamic collapse phase in which the material spreads horizontally. When the rate of spreading becomes less than spreading due to turbulent diffusion, the final transport-diffusion phase of transport begins. An idealization of all three phases of the short-term disposal are shown in Figure 18.

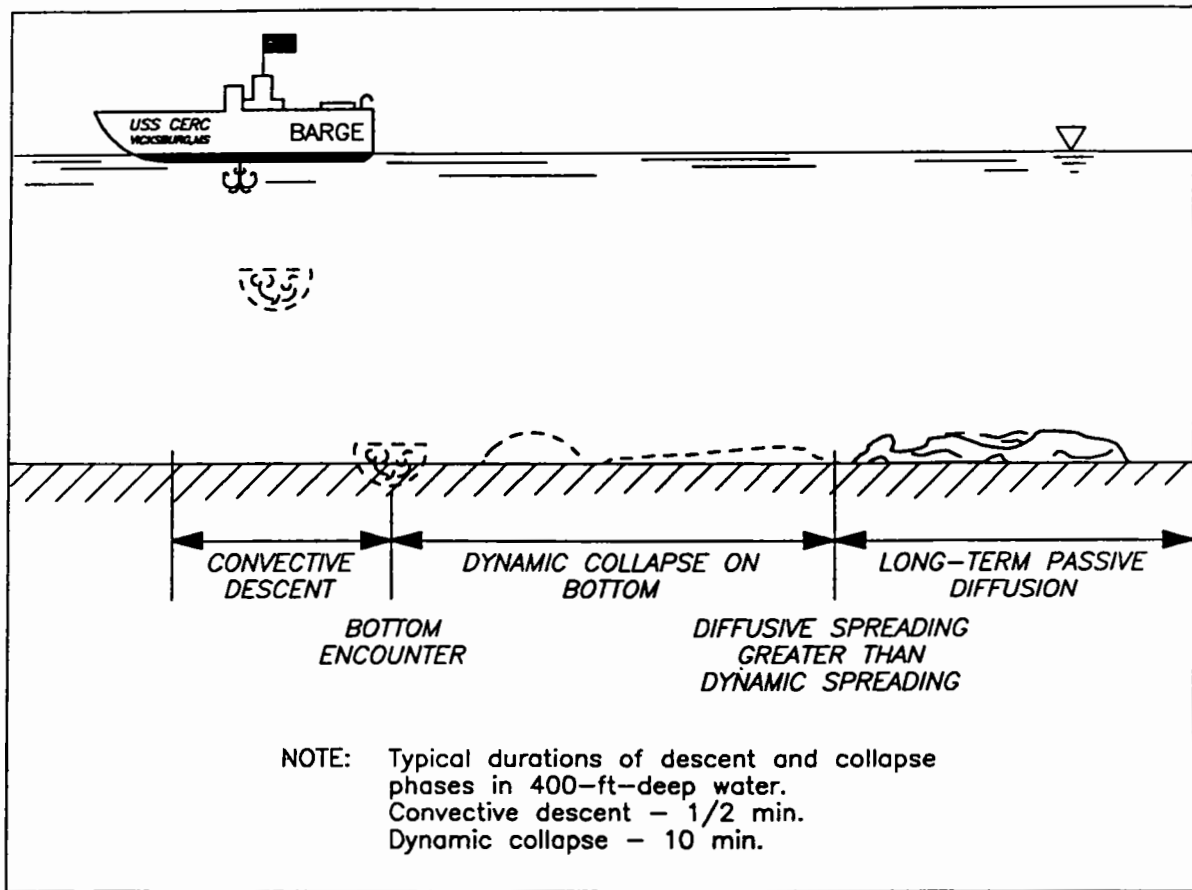


Figure 18. Computational phases of the DIFID Model
(from Brandsma and Divoky 1976)

Input Data Requirements

26. The DIFID model requires site-specific input data to quantitatively predict the short-term sediment fate of a disposal operation. These data include the physical dimensions of the dredge, a description of the local environment (depth and velocity field), a knowledge of the composition and characteristics of the material in the dredge, and specification of the numerous modeling parameters and coefficients.

27. In this particular case, inner harbor dredged material was separated into two groups based on sediment size. The coarse and fine material had a constituent breakdown of 15/85 and 85/15 percent silt-clay/ sand, respectively. Additionally, the two main components of the mean depth-averaged current system (northeast-southwest and northwest-southeast) were

applied to the model. Based on the combination of various model input parameters, four case studies are performed. They include:

- a. Case 1: Worst-case depth-averaged northeast-southwest current speed of 1.5 ft/sec and fine-grained sediment.
- b. Case 2: Worst-case depth-averaged northwest-southeast current speed of 1.0 ft/sec and fine-grained sediment.
- c. Case 3: Worst-case depth-averaged northeast-southwest current speed of 1.5 ft/sec and coarse-grained sediment.
- d. Case 4: Worst-case depth-averaged northwest-southeast current speed of 1.0 ft/sec and coarse-grained sediment.

28. Model input requires specification of the size and capacity of the dredge. It is anticipated that 70 percent of dredging operations will involve a "Manhattan" class dredge, or one of similar dimensions.* This dredge will deposit material in approximately 45 to 55 ft of water. Because the DIFID model assumes a single load disposal, it is assumed that the entire volume of a Manhattan class hopper dredge is released at once. Although this assumption may not be entirely accurate, results give a worst case scenario from which disposal decisions can be based. Capacities and dimensions of the Manhattan class dredge are given in Table 5.

Table 5

Capacities and Dimensions of the Manhattan Class Dredge

Overall length	280 ft
Width	52 ft
Depth	21.5 ft
Unloaded draft	8 ft
Loaded draft of vessel	19.4 ft
Volume	3,000 cu yd

29. Additional site-specific parameters include the specification of grid resolution Δx , total simulation duration T_d , and the long-term time-step Δt . Parameter estimation is presently based on a review of previous case studies and the ongoing DIFID model sensitivity investigation. Values for the internal model coefficients were based on recommendations and

* Personal Communication, Dec 1990, B. Kyzer, USAE District, Charleston, Charleston, SC.

Table 6
Model Input Parameters and Coefficients

Variables	Values
Grid size, Δx (ft)	100
Number of cells:	
Cross-shore direction	105
Alongshore direction	28
Time-step, Δt (sec)	80
Duration of simulation, T_d (sec)	8,000 (fine-grained site)
Duration of simulation, T_d (sec)	8,000 (coarse-grained site)
Ambient velocity (cm/sec)	
Cases 1 and 3	45.7
Cases 2 and 4	30.5
Local depth (ft)	65.0 (fine-grained site)
	65.0 (coarse-grained site)
X-Direction (on-offshore)	
bottom slope (deg)	0.00
Y-Direction (alongshore)	
bottom Slope (deg)	0.00
Ambient density (gm/cc)	1.018
DINCR1	1.0
DINCR2	1.0
Entrainment coefficient ALAPHO	0.235
BETA	0.0
CM	1.0
Drag coefficient for sphere, CD	0.5
GAMA	0.25
Drag coefficient for elliptic	
cylinder, CDRAG	1.0
CFRIC	0.01
CD3	0.10
CD4	1.00
ALPHAC	0.0010
Bottom friction, FRICTN	0.0100
FI	0.10
ALAMDA	0.005
AKYO	0.05

applications reported by Johnson (1990) and Johnson and Holiday (1978). The parameters and coefficients used in both simulations are shown in Table 6.

30. Final input to the DIFID model is the specification of the composition of the solid material in the dredge according to percent volume of sand, clay and silt, clumps, rocks, etc. Each component must be defined according to its respective density, concentration by volume, fall velocity, and voids ratio. The percent distribution of the coarse sediments was an 85/15-percent

distribution of sand/silt-clay, whereas the fine sediments contained a 15/64/21-percent distribution of sand/silt-clay/clay-clumps.* These percentages represent only the solids portion of the material. The total fluid composition of each sample was based on a separate percent distribution computation for the water content of the sand portion and the silt-clay portion. The coarse materials were defined to contain 68-percent solids, of which 85 percent is sand and 15 percent is silt-clay. The fine-grained samples were defined as 42-percent solid, with 15-percent sand and 85-percent silt-clay. The silt-clay component is further separated into a mixture of 75-percent suspendable material and 25-percent clumps. Final results of the computations are shown in Table 7 for the fine-grained material and in Table 8 for the coarse-grained material.

Table 7
Fine-Grained Sediment Composition and Characteristics

<u>Description</u>	<u>Density</u> <u>g/cc</u>	<u>Volume</u> <u>percent</u>
Sand	2.600	6.3
Silt-Clay	2.600	26.8
Clumps	2.600	8.9
Water	1.018	58.0

Table 8
Coarse-Grained Sediment Composition and Characteristics

<u>Description</u>	<u>Density</u> <u>g/cc</u>	<u>Volume</u> <u>percent</u>
Sand	2.600	57.8
Silt-Clay	2.600	10.2
Water	1.018	32.0

* Personal Communication, Dec 1990, B. Kyzer, USAE District, Charleston, Charleston, SC.

These data were input to the DIFID model. Result of the computations are presented in the following sections.

Short-Term Model Simulations

31. The short-term model is employed in the selection of a disposal point within the boundaries of the designated disposal site that would minimize any disposal-related effect to the hard bottom areas. For this purpose, two properties of the disposal operation are investigated: (a) the concentration and transport characteristics of the sediment plume, and (b) the maximum horizontal distance from the disposal point at which an appreciable amount of material settles, i.e. the measureable limit of deposition. These two properties of the impact are addressed by the model during both the dredged material descent and collapse phases. During the descent phase, the size of the sediment cloud increases (diffuses) and consequently becomes less concentrated. Calculations during this phase can be used to estimate the time change in sediment concentration with depth and distance from the barge. Both concentration distribution and total deposition results are presented separately for the fine- and coarse-grained disposal operations. Lastly, due to DIFID model constraints, a disposal depth of 65 ft is employed in the simulation. By modeling the disposal operation in a 65-ft depth rather than the measured 45- to 55-ft depth, a conservative suspended sediment concentration estimate is effectively ensured.

Fine-Grained Disposal Site Analysis

32. To simulate the fine-grained disposal operation in the two worst-case current conditions, the coefficients presented previously were input to the numerical model for each of the major and minor current axes. Model results include the spatial distribution of the sand and silt-clay components of the sediment load in the form of a nondimensional ratio of volume of solids to volume of solution. To convert these values to mg/l, multiply by sediment density $(2.60) \times 10^6$. The clay-clump component of the fine material settled to the sea bottom relatively quickly; consequently, a concentration distribution is not provided. An example of transport and diffusion of the sediment cloud is shown in Figures 19 through 21, in which the horizontal distribution

of the suspended sediment concentration of the silt-clay cloud is shown at the 30-ft depth (below the surface) for the postdump times of 2,000, 4,000, and 6,000 sec. These concentration snapshots show the increase in size and corresponding decrease in concentration of the settling cloud as it is dispersed and diffused from the point of release from the barge. The point of disposal in Figures 19-21 is at grid cell 10 (0.19-mile point).

33. Results of the concentration computation are used to produce a volume ratio concentration above ambient conditions versus distance relationship along the central axis of the grid at three discrete depths for three specified time periods (i.e., along the axis of symmetry at grid 14 of Figures 19-21). Quarter-points were selected to show results at one-fourth, one-half, and three-fourths of the termination time following the initial release of material from the barge. These plots are presented only for the silt-clay component of the disposed material since the concentration of suspended sand was comparatively insignificant. In Figures 22 and 23, the concentration history plots for the silt-clay component under the influence of the worst-case mean current speeds of 1.5 (Case 1) and 1.0 (Case 2) ft/sec are presented, respectively.

34. Results shown in Figures 22 and 23 represent time-concentration histories along the suspended sediment cloud axis. The three concentration profiles shown at the 30-ft level of Figure 22 correspond to the central axis of Figures 19 through 21. The three depths of 30, 40, and 50 ft were used to demonstrate the sediment distribution through the water column. For example, simulations of the disposal operation indicate that very little suspended sediment exists in the upper 40 ft of the water column 6,000 sec after the initial dump; i.e., the material has passed through that depth. The examples presented in Figures 22 and 23 indicate that the maximum silt-clay concentration is located in the middepth region and that the silt-clay concentration decreases with both time after disposal and distance from the release point. A summary of the Cases 1 and Case 2 silt-clay concentration simulations are shown in Tables 9 and 10, respectively.

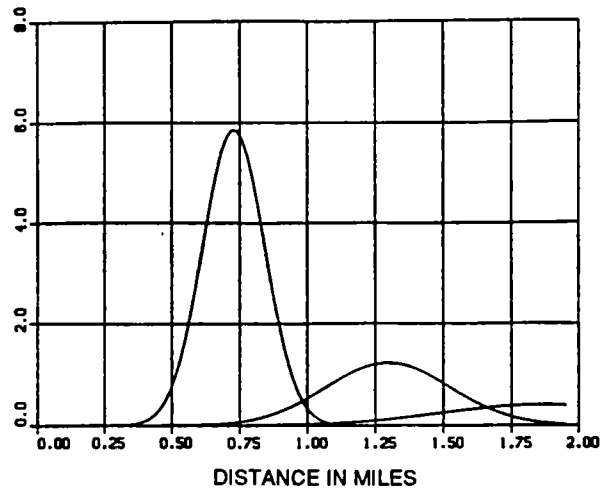
35. In Figures 24 and 25, the total sediment deposition versus distance along the axis of the disposal grid is shown for Cases 1 and 2, respectively. Additionally, a three-dimensional view of the Cases 1 and 2 deposition pattern is shown in Figures 26 and 27, respectively, with the corresponding contour plots shown in Figures 28 and 29.

[illegible]

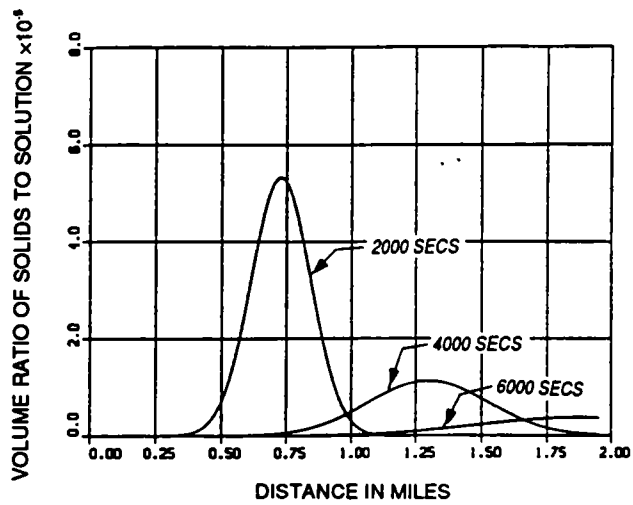
43

[illegible]

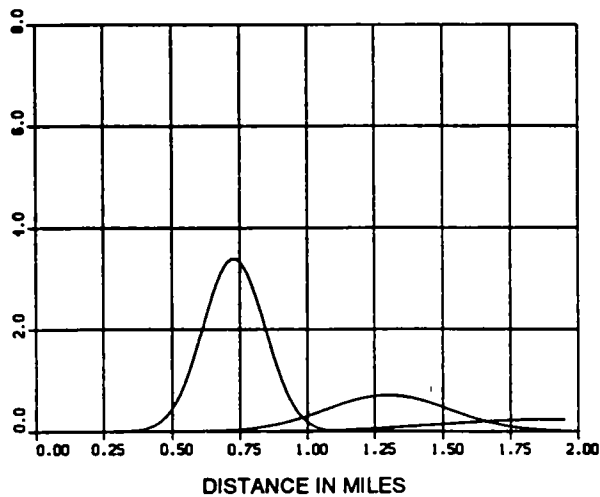
[illegible]



a. 30-ft depth

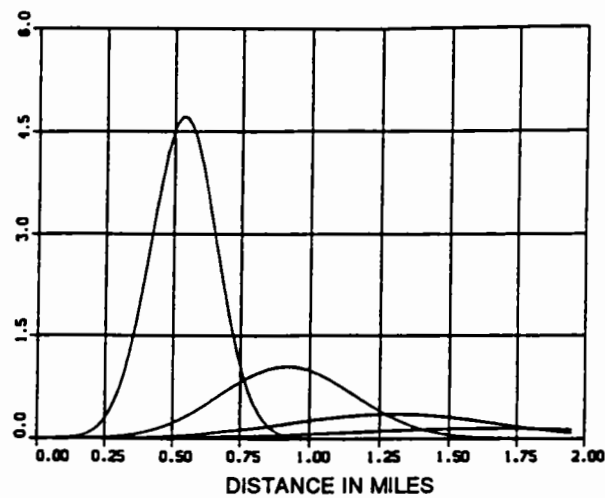


b. 40-ft depth

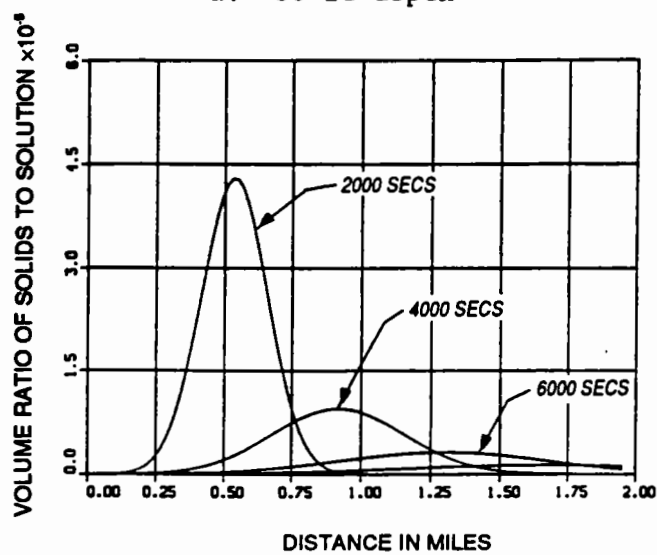


c. 50-ft depth

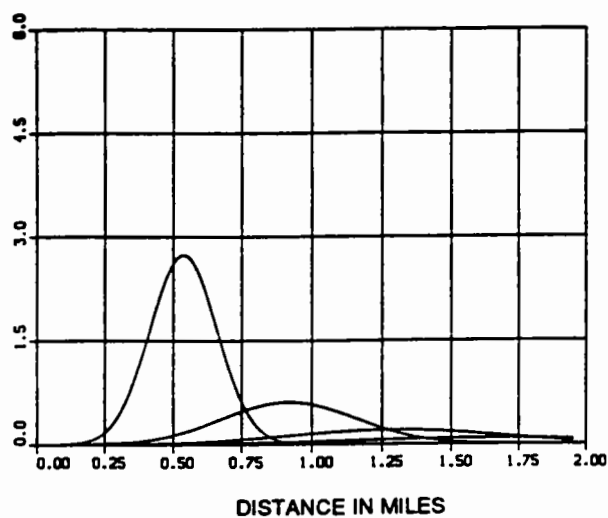
Figure 22. Silt-clay concentration evolution relationships for the fine-grained site (Case 1)



a. 30-ft depth



b. 40-ft depth



c. 50-ft depth

Figure 23. Silt-clay concentration evolution relationships for the fine-grained site (Case 2)

Table 9

Summary of Computed Maximum Suspended Silt-Clay Concentration,* Case 1

Depth, ft	Time, sec/Approximate Distance from Disposal, miles		
	2,000/0.55	4,000/1.13	6,000/1.75
30	5.8×10^{-5}	1.2×10^{-5}	4.0×10^{-6}
40	5.3×10^{-5}	1.1×10^{-5}	3.6×10^{-6}
50	3.3×10^{-5}	7.1×10^{-6}	2.3×10^{-6}

* Concentration in volume ratio of solids to solution above ambient.

Table 10

Summary of Computed Maximum Suspended Silt-Clay Concentration,* Case 2

Depth, ft	Time, sec/Approximate Distance from Disposal, miles		
	2,000/0.37	4,000/0.75	6,000/1.12
30	4.7×10^{-5}	1.0×10^{-5}	3.5×10^{-6}
40	4.2×10^{-5}	1.0×10^{-5}	3.2×10^{-6}
50	2.7×10^{-5}	6.0×10^{-6}	2.0×10^{-6}

* Concentration in volume ratio of solids to solution above ambient.

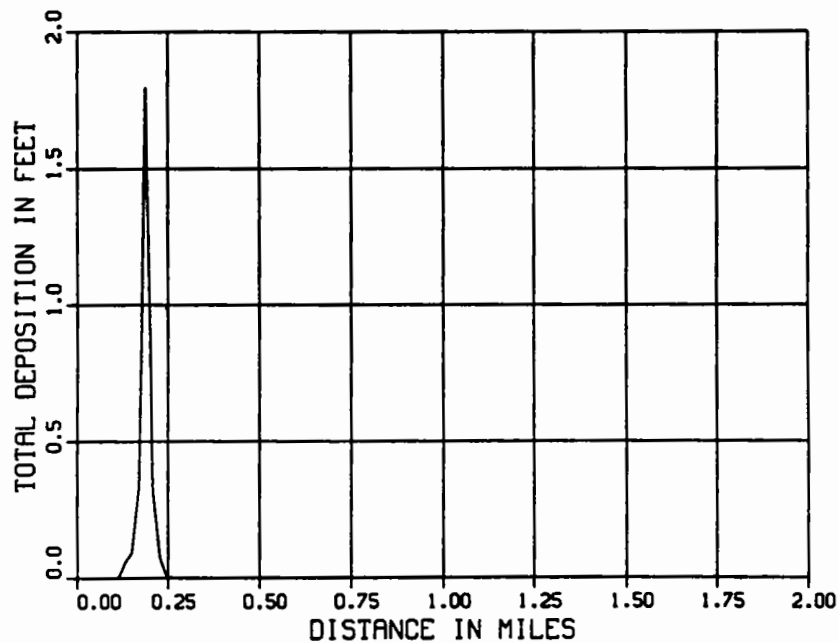


Figure 24. Total deposition pattern
for the fine-grained site (Case 1)

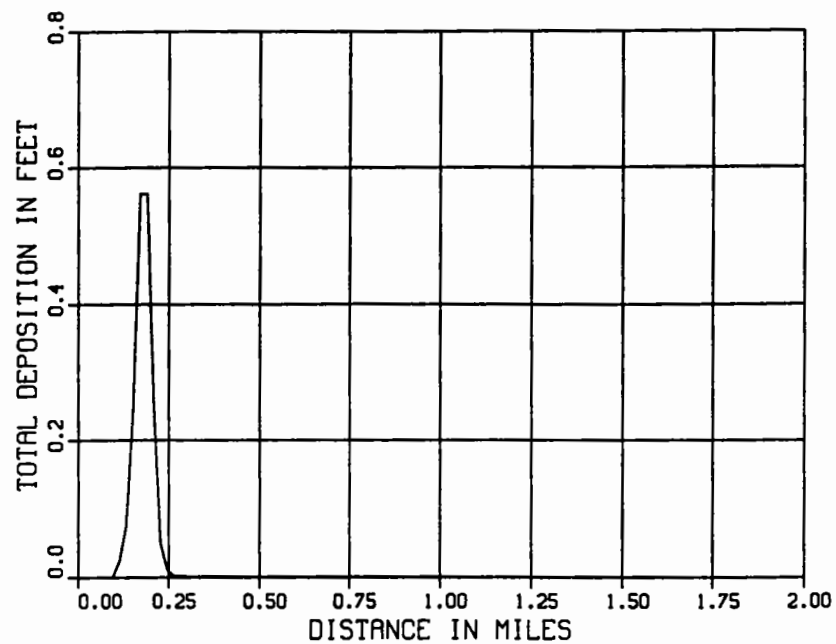


Figure 25. Total deposition pattern
for the fine-grained site (Case 2)

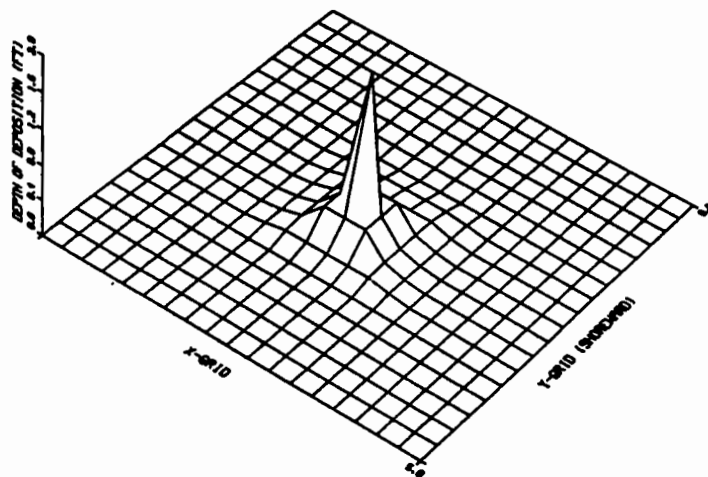


Figure 26. Three-dimensional view
of the fine-grained site deposition
pattern (Case 1)

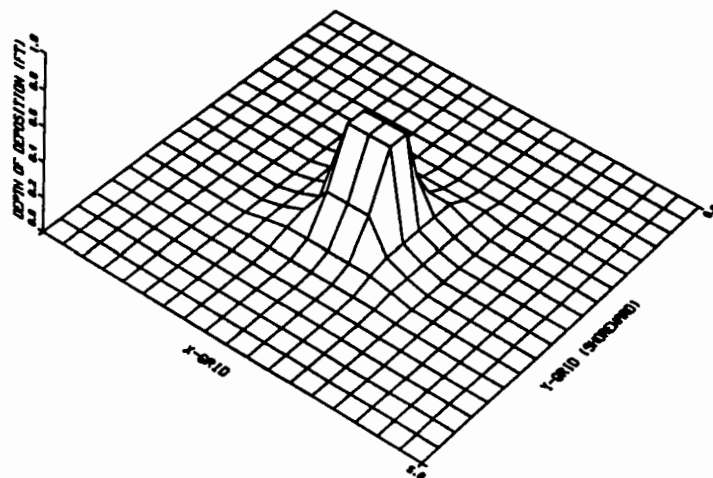


Figure 27. Three-dimensional view of the fine-grained site deposition pattern (Case 2)

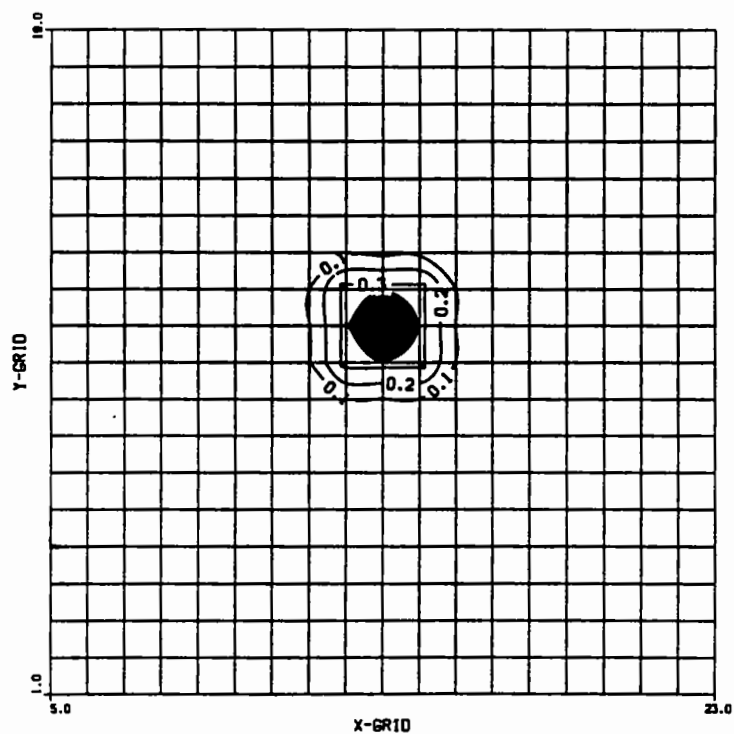


Figure 28. Contour plot of the fine-grained site deposition pattern (Case 1)

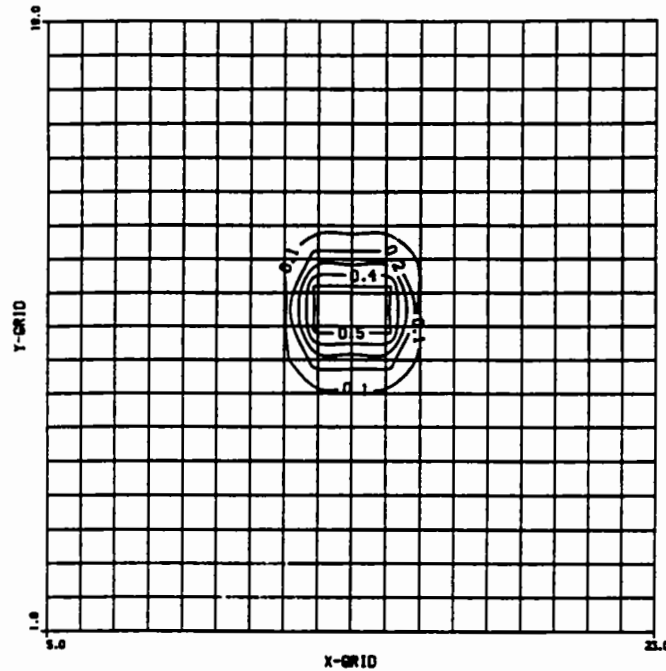


Figure 29. Contour plot of the fine-grained site deposition pattern (Case 2)

36. To aid the engineer or scientist in selecting a disposal location that would minimize the effect on hard bottom areas, plume concentration information has been compiled and is presented in Figure 30. This figure describes the evolution of depth-averaged peak plume concentration as it is advected from the disposal point. In the figure, exponential-type regression curves are given for Cases 1 and 2; the corresponding equation follows.

$$X_{(1 \text{ or } 2)} = \frac{1}{\alpha} \log_e \left[\frac{C}{\beta} \right] \quad (3)$$

Where C is the allowable silt-clay suspended sediment volume ratio concentration $\times 10^6$, and α and β are equal to -2.2 and 116 for Case 1, and -2.8 and 71 for Case 2.

37. A simple method that can be used to determine whether or not a particular disposal location meets the required minimal hard bottom effect requirements is given:

- a. Determine an acceptable suspended sediment concentration level at the location of the hard bottom.

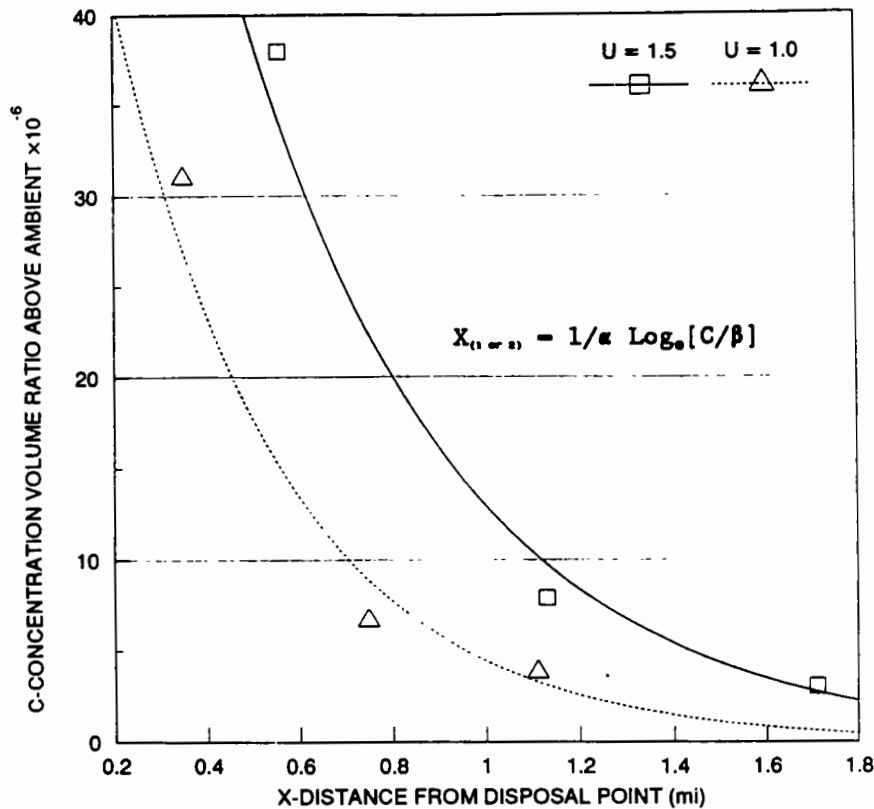


Figure 30. Evolution of depth-averaged peak plume concentration for Cases 1 and 2 of fine-grained material

- b. Determine the value of X_1 and X_2 from Figure 31 or from Equation 3.
- c. Construct an ellipse about the selected disposal point (center) with a major axis of length $2X_1$ running in the northeast-southwest direction and a minor axis of length $2X_2$ running in the northwest-southeast direction.
- d. If the hard bottom areas fall outside the boundary of the ellipse, the selected disposal location is acceptable; if not, select another disposal point and reapply this test.

Coarse-Grained Disposal Site Analysis

38. The single-load deposition simulation for the coarse-grained material was performed using the coefficients shown in Tables 6 and 8. Results of the simulations showed that the coarsest fraction of this material descended rapidly to the ocean floor, leaving no sand in suspension within the water column. The silt-clay fraction of this material, however, rapidly moved into

suspension as can be seen in Figures 31 and 32. As in the case of the fine-grained material, the concentration of silt-clay slightly increases with distance above the bottom and decreases with time. However, the maximum value of coarse-grained suspended sediment concentration is an order of magnitude less than that of the fine-grained material. A summary of the Case 3 and Case 4 silt-clay concentration simulations are shown in Tables 11 and 12, respectively. In Figures 33 and 34, the total sediment deposited versus distance along the axis of the disposal grid is shown for Cases 3 and 4, respectively.

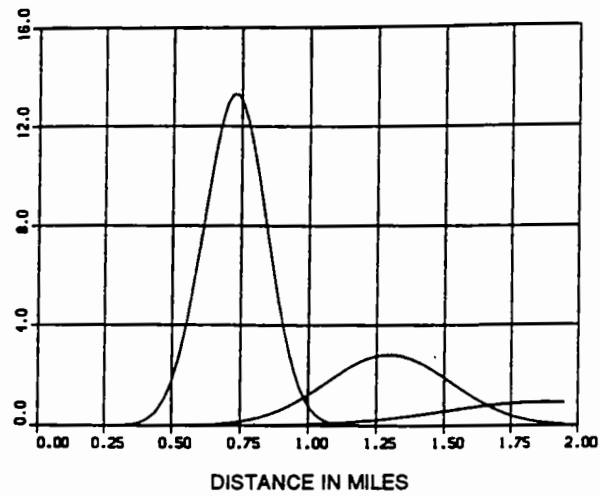
39. Additionally, a three-dimensional view of the Cases 3 and 4 deposition pattern is shown in Figures 35 and 36, respectively, with the corresponding contour plot shown in Figures 37 and 38. Based on these figures, the maximum thickness of deposition for Cases 3 and 4 is approximately 0.45 and 0.5 ft, respectively. The deposition, for both cases, covers an approximate 700-ft-diameter area. Deposition is shown to be confined to this immediate area.

40. As in the case of the fine-grained material, plume concentration information for the coarse-grained site has been compiled and is presented in Figure 39. This figure describes the evolution of depth-averaged peak plume concentration as it is advected from the disposal point. In the figure exponential-type regression curves are given for Cases 3 and 4; the corresponding equation follows.

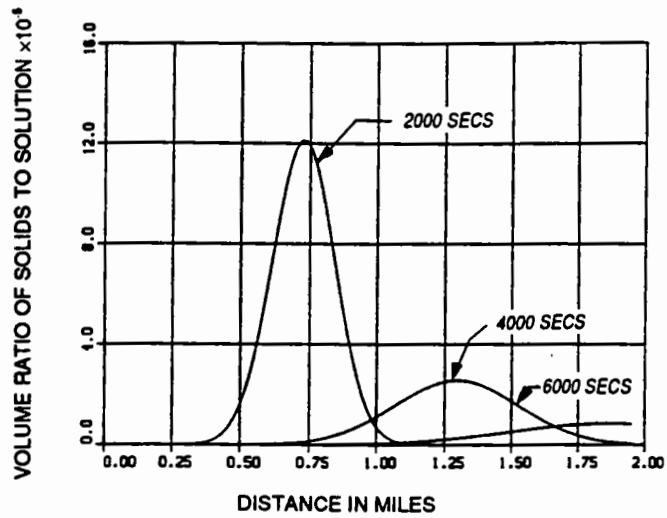
$$X_{3 \text{ or } 4} = \frac{1}{\alpha} \text{Log}_e \left[\frac{C}{\beta} \right] \quad (4)$$

where C is the allowable silt-clay suspended sediment volume ratio concentration $\times 10^6$, and α and β are equal to -2.5 and 35 for Case 3, and -4.8 and 52 for Case 4.

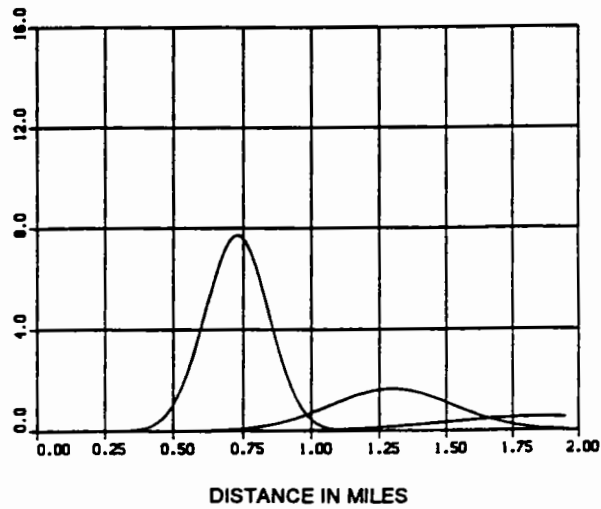
41. In both the fine- and coarse-grained DIFID analyses, depth-averaged velocities of 1.5 and 1.0 ft/sec were assumed as a conservative estimate of the northeast-southwest and northwest-southeast velocity component, respectively. As shown in the prototype data analysis, these velocity magnitudes represents a much higher-than-average condition, and, as such, the results presented for the short-term simulation may be considered conservative with respect to the dispersion of the suspended sediments. An analysis of the



a. 30-ft depth

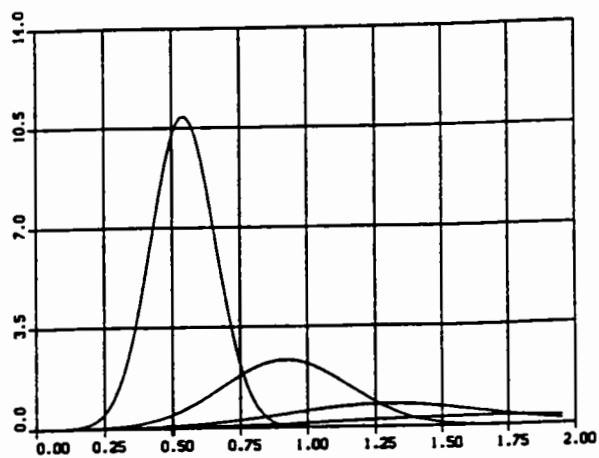


b. 40-ft depth

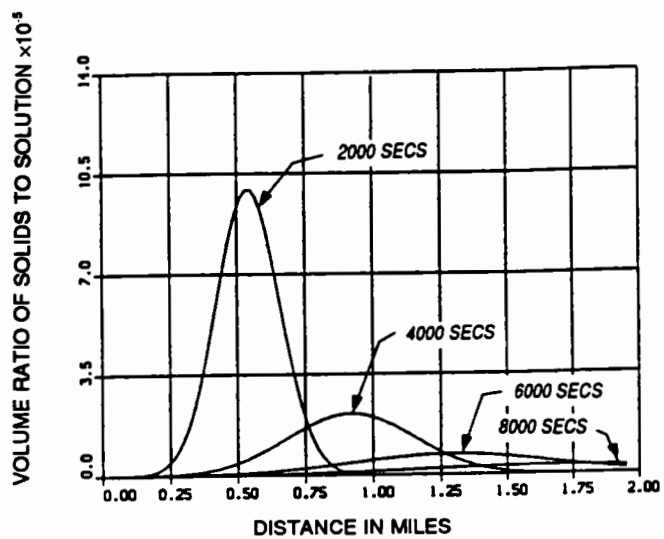


c. 50-ft depth

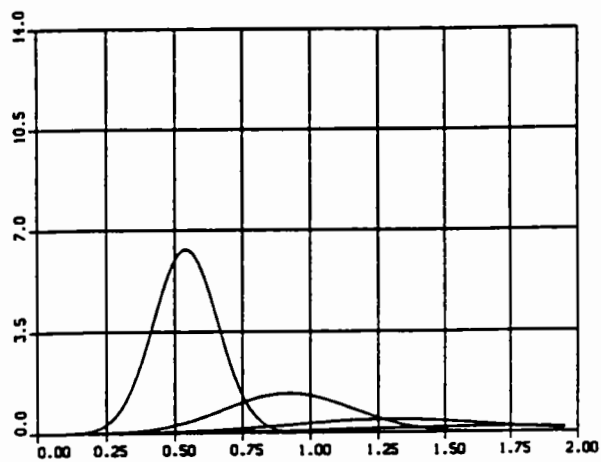
Figure 31. Silt-clay concentration evolution relationships for the coarse-grained site (Case 3)



a. 30-ft depth



b. 40-ft depth



c. 50-ft depth

Figure 32. Silt-clay concentration evolution relationships for the coarse-grained site (Case 4)

Table 11

Summary of the Computed Maximum Suspended Silt-Clay Concentration,* Case 3

<u>Depth, ft</u>	<u>Time, sec/Approximate Distance from Disposal, miles</u>		
	<u>2,000/0.50</u>	<u>4,000/1.12</u>	<u>6,000/1.70</u>
30	1.3×10^{-5}	2.8×10^{-6}	9.2×10^{-7}
40	1.2×10^{-5}	1.5×10^{-6}	8.4×10^{-7}
50	7.7×10^{-6}	1.6×10^{-6}	5.1×10^{-7}

* Concentration in volume ratio of solids to solution above ambient.

Table 12

Summary of Computed Maximum Suspended Silt-Clay Concentration,* Case 4

<u>Depth, ft</u>	<u>Time, sec/Approximate Distance from Disposal, miles</u>		
	<u>2,000/0.54</u>	<u>4,000/0.76</u>	<u>6,000/1.14</u>
30	1.0×10^{-5}	2.3×10^{-6}	7.8×10^{-7}
40	1.0×10^{-5}	2.1×10^{-6}	7.1×10^{-7}
50	6.3×10^{-6}	1.3×10^{-6}	4.5×10^{-7}

* Concentration in volume ratio of solids to solution above ambient.

short-term analysis results will be presented following the long-term simulations described in Part IV.

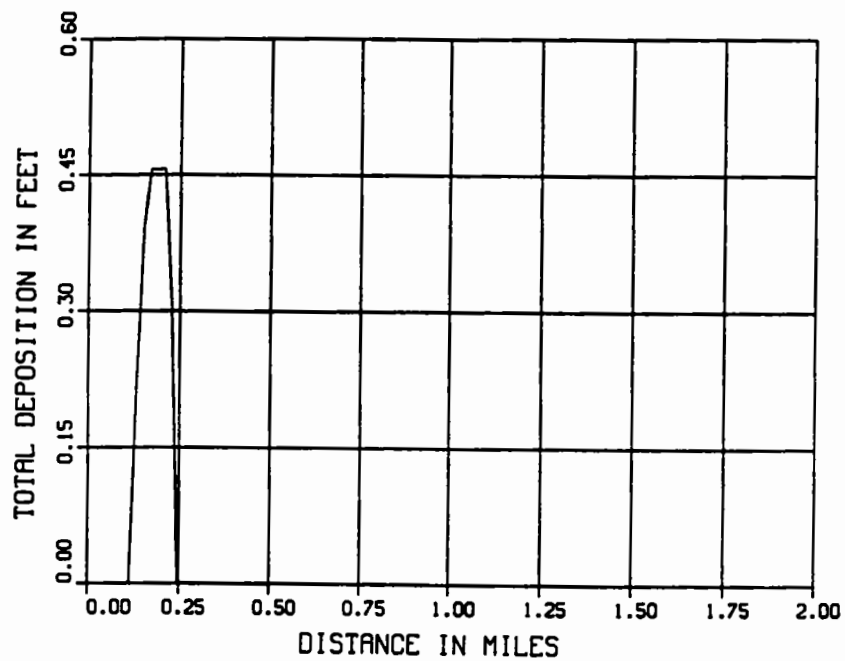


Figure 33. Total deposition pattern for the coarse-grained site (Case 3)

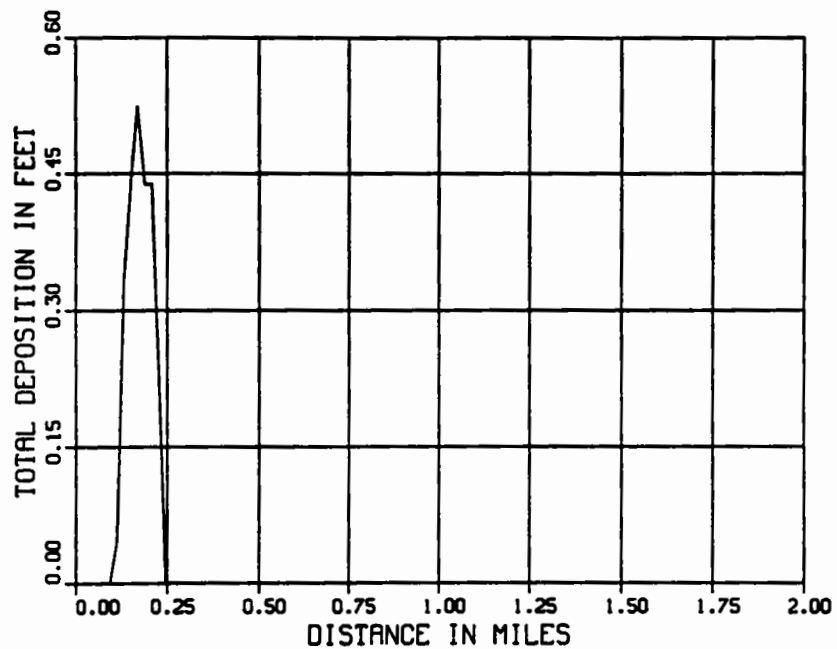


Figure 34. Total deposition pattern for the coarse-grained site (Case 4)

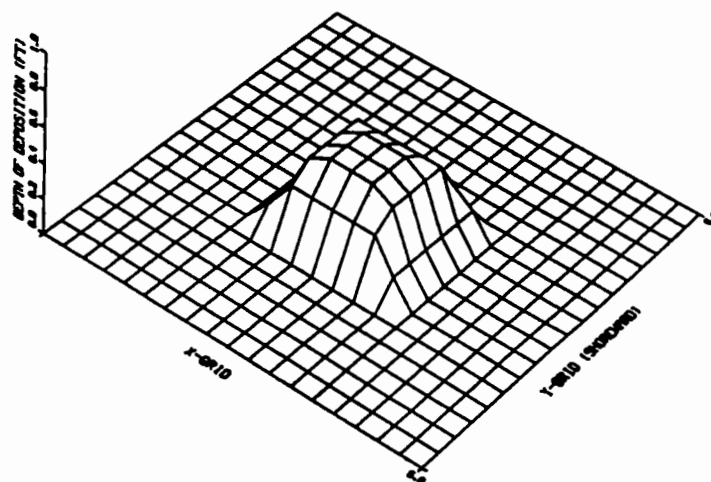


Figure 35. Three-dimensional view of the coarse-grained site deposition pattern (Case 3)

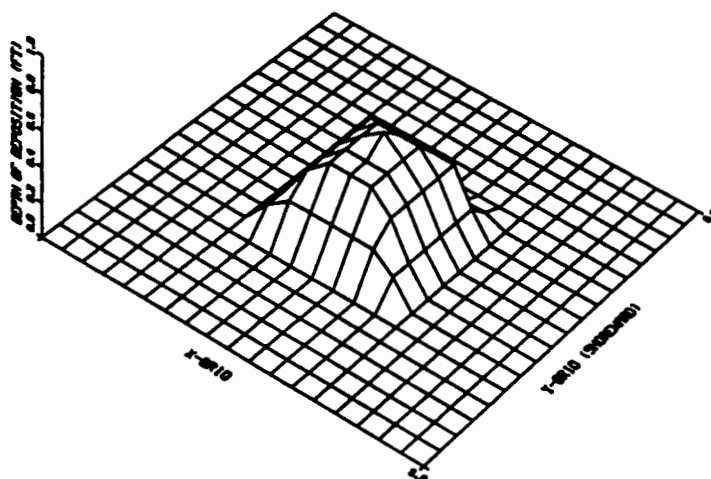


Figure 36. Three-dimensional view of the coarse-grained site deposition pattern (Case 4)

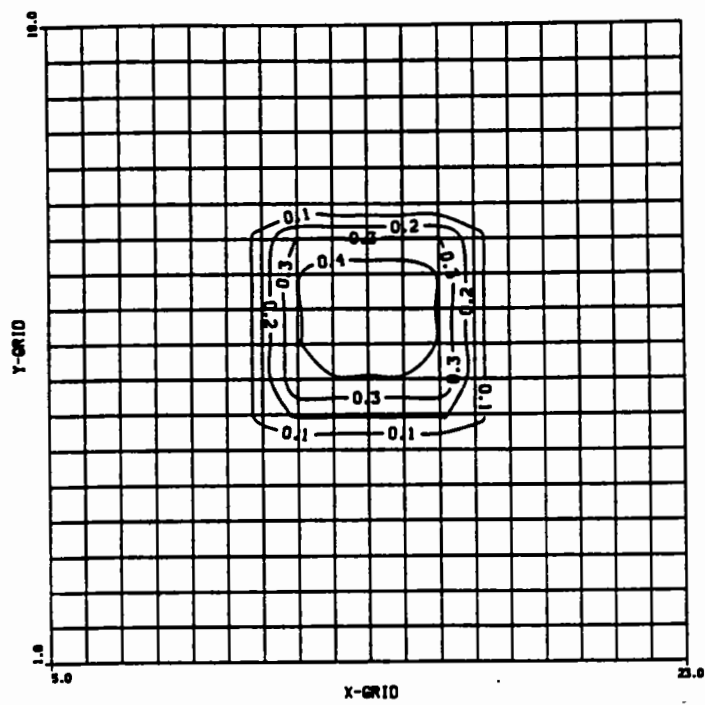


Figure 37. Contour plot of the coarse-grained site deposition pattern (Case 3)

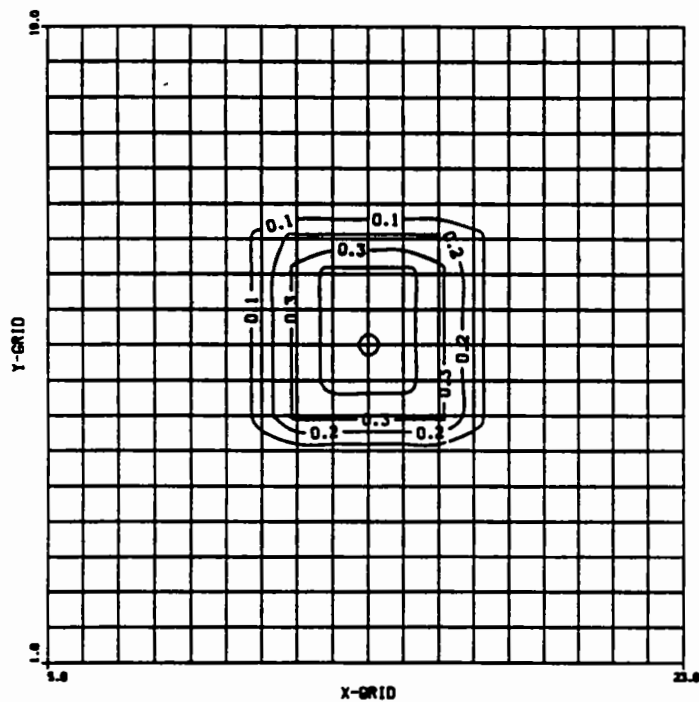


Figure 38. Contour plot of the coarse-grained site deposition pattern (Case 4)

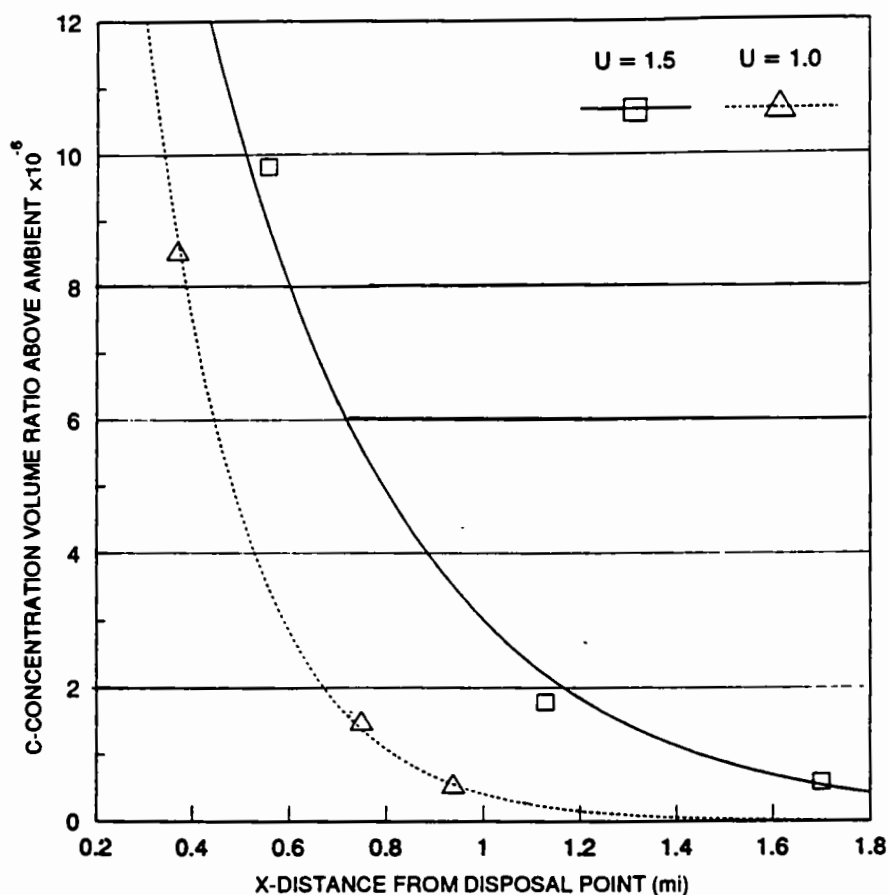


Figure 39. Evolution of depth-averaged peak plume concentration for Cases 3 and 4 of fine-grained material

where C is the allowable silt-clay suspended sediment volume ratio concentration $\times 10^6$, and α and β are equal to -2.5 and 35 for Case 3, and -4.8 and 52 for Case 4.

41. In both the fine- and coarse-grained DIFID analyses, depth-averaged velocities of 1.5 and 1.0 ft/sec were assumed as a conservative estimate of the northeast-southwest and northwest-southeast velocity component, respectively. As shown in the prototype data analysis, these velocity magnitudes represents a much higher-than-average condition, and, as such, the results presented for the short-term simulation may be considered conservative with respect to the dispersion of the suspended sediments. An analysis of the short-term analysis results will be presented following the long-term simulations described in Part IV.

PART IV: LONG-TERM MODELING

General

42. The long-term simulation phase of the site characterization study investigates the behavior of a dredged material mound over time. This analysis is accomplished by developing a means of classifying disposal sites as either dispersive or nondispersive based on whether local wave and velocity fields are adequate to erode and transport significant amounts of material from the site. The local currents can be due to normal tidal action and mean flow circulation patterns or storm-related activity. Sediment transport calculations use these waves and currents to estimate mound stability as a function of the local bathymetry and sediment characteristics at both the fine-grained and coarse-grained sites. The transport relationships used for this study were limited to noncohesive sediments. Although a majority of the fine grained sediments are classified as silt/clay, they contain approximately 15% sand. The assumption was made that the overall material behaves in a noncohesive manner and can be approximated with noncohesive relationships. This assumption is consistent with results presented by Kamphius (1990) stating that "If sand or gravel is presented in the eroding stream or overlying the cohesive formation in a discontinuous layer, the design should be based on the sediment transport characteristics of the granular material." Details of the specified grain sizes for the coarse and fine grained sediments are presented below under Input Data Requirements.

43. This final phase of the site evaluation represents an extension of the short-term fate analysis of Part III in which site dispersiveness was based on the ability to effectively place material within a designated site during the disposal operation. The long-term analysis begins with the assumption that the short-term disposal operation is successful in creating a stable mound configuration. Whether the mound is dispersive or nondispersive depends on whether the local wave and current conditions are capable of resuspending and transporting significant amounts of material from the mound such that areas adjacent to the disposal site are affected.

44. The long-term site stability analysis approach adopted for this study uses the simulated wave and current time series described in Part II to provide a quantitative estimate of the stability of the mound as a function of localized environmental conditions. The analysis approach is based on coupled

hydrodynamic and sediment transport models that compute the transport of noncohesive sediment as a function of the local velocity and depth. The resulting distribution of transport is used in a sediment continuity model to compute changes in the bathymetry of the sediment mound. Bathymetry change computations are made at every 3-hr time-step. The long-term simulations of mound stability indicate whether the local wave and current regime at the disposal site are of sufficient magnitude to suspend and transport bottom sediments.

Input Data Requirement

45. The site stability methodology is dependent on the accurate prediction of sediment transport at the site under investigation. Empirical relationships for computing sediment transport as a primary function of depth-averaged water velocity, local depth, and sediment grain size were reported by Ackers and White (1973). A modification of the transport equations was introduced to reflect an increase in sediment transport rate when ambient currents are accompanied by surface waves. The modification, in the form of an effective increase in the depth-averaged current, is based on concepts developed by Bijker (1967) and implemented by Swart (1976). This additional transport reflects the fact that wave-induced orbital velocities are capable of suspending bottom sediments, independent of the sediment put in suspension by mean currents. The total amount of sediment put into suspension by waves and currents is then transported by the ambient current field.

46. The modified Ackers-White relationships are used to compute the transport of uniformly graded noncohesive sediment in the grain diameter (D_{50} for example) range of 0.04 to 4.00 mm (White 1972). Consequently, D_{50} values of 0.100 and 0.063 mm were selected to represent the fine sand and silt-size sediments to be deposited at the ODMDS. Computed sediment transport versus depth-averaged velocity for a range of depths corresponding to those at the coarse-grained site are shown in Figures 40 and 41 for the D_{50} values of 0.100 and 0.063 mm, respectively. The WIS summary mean wave height of 0.5 m and wave period of 3.9 sec were specified in the preparation of this family of curves. From these two figures, the threshold velocities necessary for the initiation of sediment erosion is almost identical for both sediment sizes, i.e. $1.0 < U < 1.5$ ft/sec.

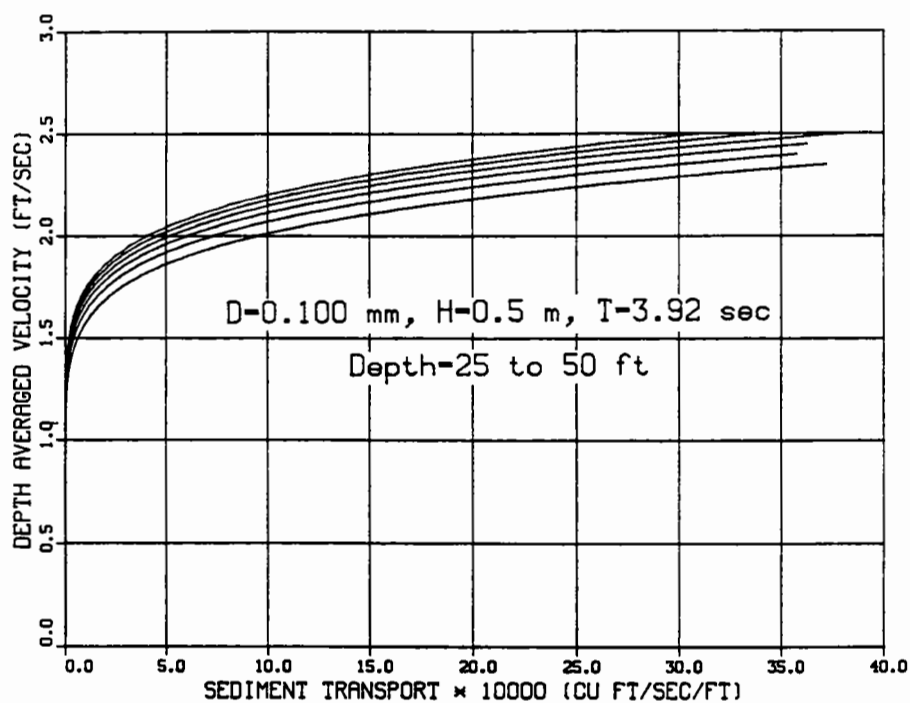


Figure 40. Sediment transport-velocity relationships
for $D_{50} = 0.10$ mm

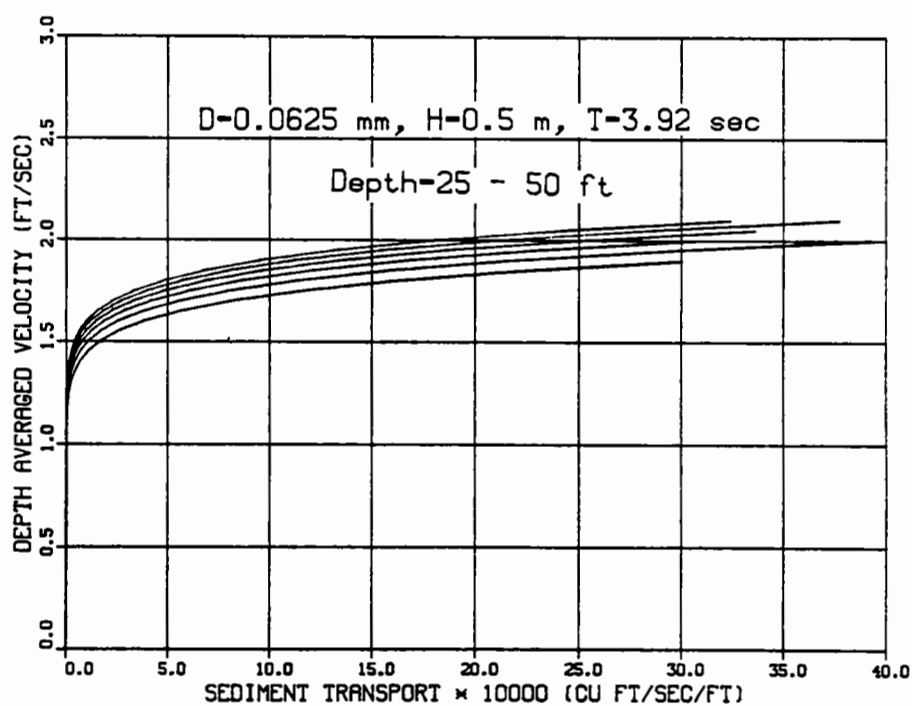


Figure 41. Sediment transport-velocity relationships
for $D_{50} = 0.0625$ mm

47. The simulated wave and current boundary condition time series at the disposal site are used to evaluate the dispersive/nondispersive characteristics of the site. This computation requires the specification of the geometric features of a typical or existing disposal mound located within the limits of the designated site. The disposal procedures followed at the Charleston ODMDS are to dispose material in parallel mounds at a spacing of approximately 300 ft. Typical mounds have a width of approximately 1,000 ft and a length of up to 5,000 ft. Heights of the elongated features are limited so that depths do not become less than approximately 30 ft.* Average depths within the site are on the order of 35 to 40 ft; therefore, a local depth of 37 ft was specified for the long-term simulations. A symmetric design mound configuration of 1,000 by 1,000 ft with a height of 7 ft was specified as a means of predicting maximum erosion rates. For example, computed migration rates along the long axis of the elongated mound would be minimal if the current was aligned with the long axis. By specifying a symmetric mound, maximum migration rates are computed because directional effects are minimized. A three-dimensional perspective view and contour map of the test mound are shown in Figures 42 and 43.

Long-Term Model Simulations

48. The long-term analysis described in the following section uses wave and velocity time series to compute the time evolution of a dredged material mound. A quantitative assessment of mound stability is made by computing the location of the centroid of the mound along the central mound axis for each computational time step of the simulation. These computations are made by balancing the summation of moments at each computational grid. Simulation results are also presented in the form of postsimulation perspective and contour plots as well as time evolution plots of the changing cross-sectional profile along the axis of the mound.

49. The stability analysis is made by estimating mound response to long periods of exposure to the wave and current conditions described in Part II. In addition to this normal condition simulation, a storm event analysis was performed in an attempt to investigate single-event-related erosion of the

* Personal Communication, Nov 1991, S. Morrison, USAE District, Charleston, Charleston, SC.

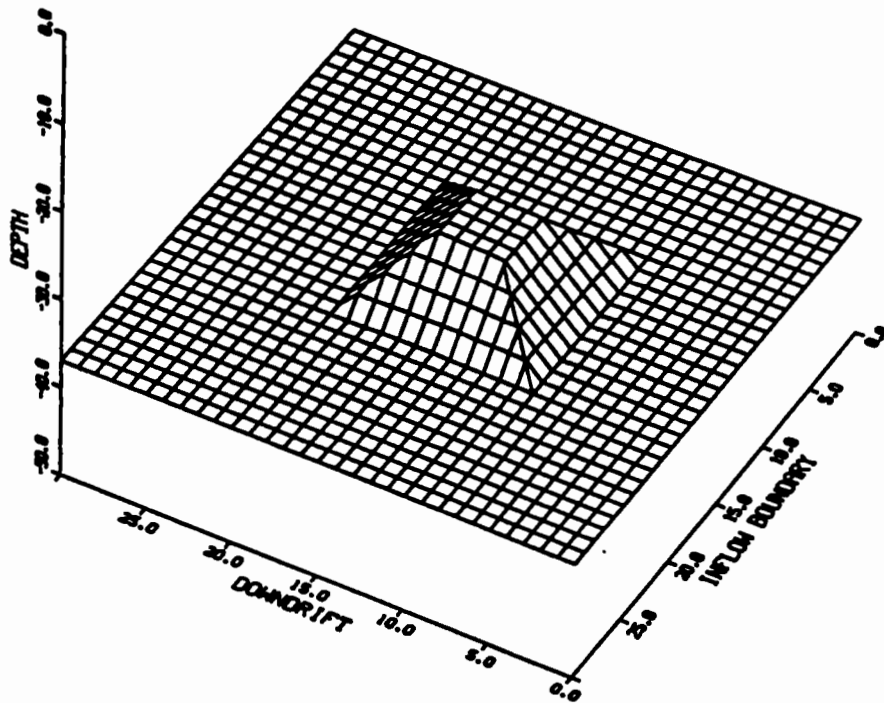


Figure 42. Idealized disposal mound perspective view

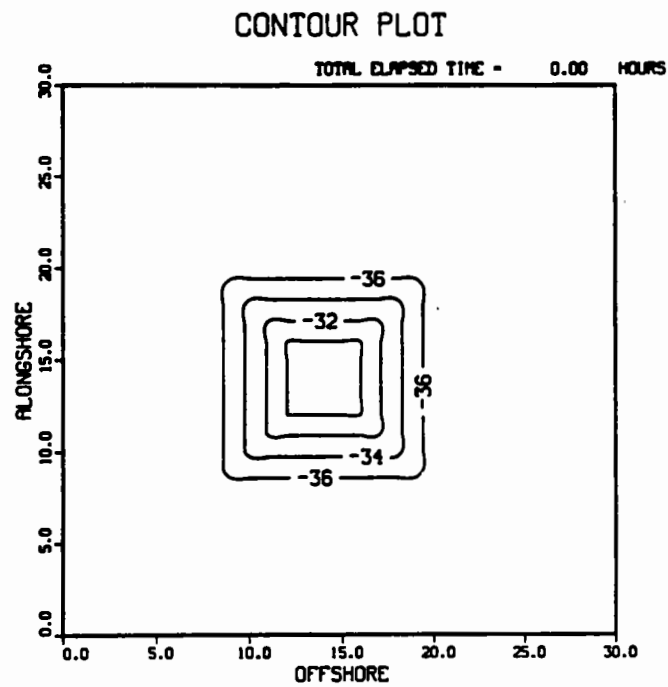


Figure 43. Idealized disposal mound contour map

test mound. A design storm event was selected with a half-sine wave shape, with a duration of 24 hr and a peak depth-averaged velocity of 2.0 ft/sec. A storm of this sustained magnitude and duration could be descriptive of a moderate northeaster or hurricane event.

50. Two long-term simulations were made to investigate the stability of a disposal mound composed of two different sediment sizes. The first simulation specified a grain size of 0.100 mm, corresponding to a fine sand; the second specified a diameter of 0.063 mm, corresponding to a noncohesive sediment approaching the silt/clay size. A 2-mo simulation of each sediment size was performed to test the design mound stability to the wave field shown in Figure 3 and the current fields described by the constituents listed in Table 3. Results of both simulations indicate that the mound experiences erosion and migration under the forces associated with normal tidal and circulation action. A migration rate of approximately 15 and 60 ft/mo were computed for the 0.100- and 0.063-mm sediments, respectively. These results show that the long-term direction of migration is to the northeast, along the major tidal current ellipse and in the direction consistent with computed average flows. Although the current records used in the reconstruction of the current time series were based on data of limited duration, the computed magnitudes and directions are realistically descriptive of normal conditions at the ODMDS. It is unlikely that longer duration current data would show results that are substantially different from those shown in the present analysis. Also, the computed magnitude and direction patterns for the NOAA sites are consistent with comparable computations for the five samples at the EPA site. Therefore, it can be reasonably concluded that the currents shown in Figure 14 are representative of the site and that these forcings are adequate to transport material from the disposal mound. In view of the repetitive nature of the velocity field and the fact that the imposed wave field corresponds to the high energy winter period beginning 1 January of the simulated year, simulations of longer than 2 months were not necessary.

51. The long-term simulation indicates that the test mound is dispersive whenever the current magnitudes exceed approximately 1.5 ft/sec; however, normal conditions are not sufficiently severe to cause massive erosion. Therefore, the mound was subjected to velocity and wave field conditions to determine the levels of severity of erosion that could be anticipated from a storm event of moderate intensity. The specified storm could be a northeaster or hurricane; therefore, the current hydrograph could be from any

direction. Results of the storm surge simulation show the mound to migrate 155 ft, many times the erosion rate associated with normal waves and currents. The fine-grained mound (0.063 mm) was used for the storm simulations to represent a worst-case erosion scenario. A plot of the poststorm simulation perspective and contour map of the mound and the computed cross-sectional evolution of the mound axis are shown in Figures 44 and 45.

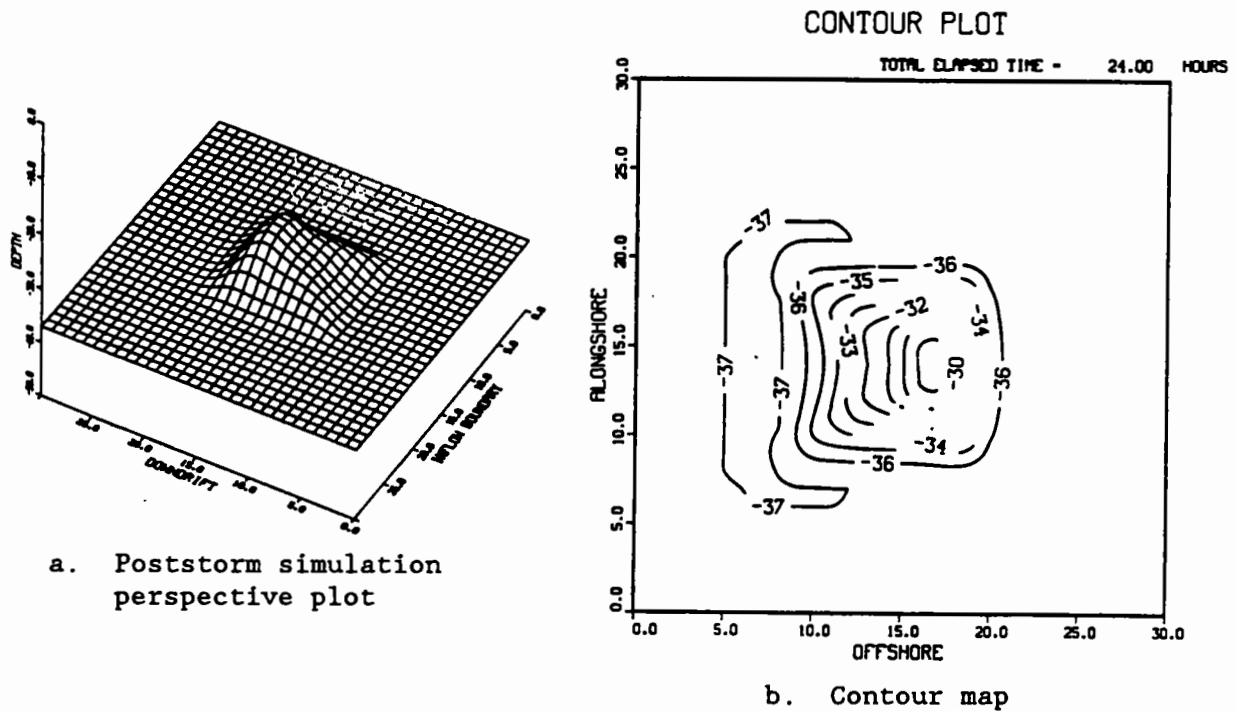


Figure 44. Storm-event simulation perspective and contour map

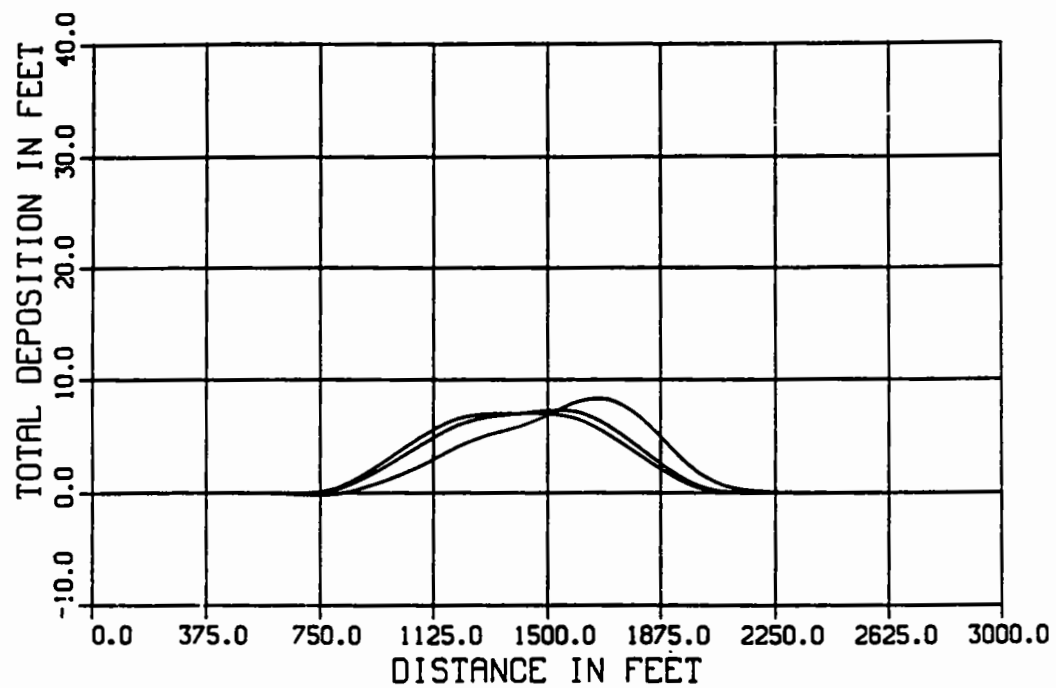


Figure 45. Storm-event simulation mound axis migration history

PART V: CONCLUSIONS

52. A dispersion analysis of the Charleston ODMDS was conducted by CERC, WES, to quantify the dispersive character associated with disposal of dredged material at the existing site. Of specific concern was whether or not the disposal operation could pose a threat to recently discovered hard bottom reef communities located within the boundaries of the existing site. The dispersion analysis was conducted in two phases. First, a short-term analysis was performed in which the immediate effects of the disposal operation were investigated by computing the spatial limits of sediment deposition on the ocean bottom and the time rate of change of suspended sediment concentrations within the water column. Second, a long-term analysis was conducted to determine whether local waves and currents were sufficiently severe to erode and transport significant amounts of material from the existing disposal mound onto the hard bottom reef areas. Both short- and long-term analyses are based on numerical model predictions using site-specific wave and current boundary conditions developed through analysis of existing data. The phases of data analysis and short- and long-term modeling are summarized in the following section.

Prototype Data Analysis

53. Although the Charleston ODMDS is reasonably dispersive, the goal of this investigation was to quantify the direction and magnitude of sediment transport with respect to the point of disposal. This goal requires an investigation and analysis of the local waves and currents that are responsible for eroding and transporting material from the site. Wave field data for this purpose were obtained from the Phase III WIS 20-year hindcast data base for a WIS station located offshore of the entrance to Charleston Harbor. Two sources of velocity data were located that were of sufficient quality that reliable estimates of current magnitude and direction at the site could be computed. The sources of data were the NOAA and the EPA. Both data sets were analyzed, and comparable results were obtained indicating that currents at the site are tidally dominated with a maximum major axis current amplitude of 40 to 50 cm/sec to the northeast-southwest and a minor amplitude axis of approximately 25 cm/sec oriented in a northwest-southeast direction. Mean values were on the order of less than 10 cm/sec in a generally northeasterly

direction. Although the data used for this analysis were limited in duration, the results are sufficiently accurate for the dispersion computations. Since the disposal site is located in relatively shallow water, i.e. less than 45 to 55 ft, the occurrence of even moderate storm events can have a greater erosional impact on the mound than those attributed to normal conditions. For this reason, a storm event analysis was included to quantify the degree of long-term storm-related erosion.

Short-Term Analysis

54. Two sediment compositions were specified in the short-term dispersion analysis, a disposal load composed of predominantly sand and one of predominately silt and clay. Results of the short-term analysis indicate that both the sand and silt/clay materials fall rapidly to the ocean floor and do not affect regions beyond 1.5 miles from the point of disposal. Computations of the movement and dispersion of the suspended sediment cloud at the 1.5 mile point indicate that maximum depth-averaged sediment concentrations in ratios of volume of solids to volume of solution above ambient (background) conditions are on the order of 3.0×10^{-6} . Concentrations at this level are equivalent to 7.8 mg/l and correspond to the predominantly silt/clay sediment. The corresponding value for the fine sand is 7.5×10^{-7} (2.0 mg/l), approximately 1.5 miles from the point of release. Figures 30 and 39 provide guidance for locating disposal positions that minimize any suspended sediment impact to the live reef area. As shown in both figures, disposal locations can be located that do not significantly affect the reef area. For example, near-reef disposal could be made during ebb flow when currents are to the northeast. When currents are reef-directed, neither the sand nor the silt/clay materials pose a problem if the disposal site is greater than approximately 1.5 miles from the reefs.

Long-Term Analysis

55. Long-term simulation of disposal mound stability was based on numerical mound stability computations based on site-specific wave and current boundary condition data. Two design sediment mounds were tested, one corresponding to a fine sand (0.100 mm) and one to a finer-grained sediment (0.063 mm). The calculations are based on the modified Ackers-White equations

of transport for noncohesive sediment. Simulations showed that both sediment mounds were dispersive with respect to normal wave and tidal/circulation currents, with migration rates on the order of 15 and 60 feet/month for the sand and fine-grained sites, respectively. Both results indicate movement to the northeast, consistent with computed current averages.

56. Since the ODMDS is located in shallow water, effects of a storm-velocity field were simulated to demonstrate the effects of storm-related erosion. The simulation of a moderate-intensity event (2 ft/sec) with a 24-hr storm showed the migration of a 0.063-mm noncohesive sediment mound to be approximately 155 ft. Since storm currents can be directed in virtually any direction, it can be seen that long-term erosion can easily be storm dominated. Computed migration rates do not, however, indicate rapid and massive erosion that would affect areas far removed from the mound. Therefore, as long as the disposal mounds are located a reasonable distance to the northeast of the reef area, no significant long-term effect to the reef area should be experienced.

Concluding Remarks

57. In conclusion, both short- and long-term analyses of the Charleston ODMDS showed that the site is moderately dispersive and that the primary direction of dispersion and erosion is to the northeast. Computations presented herein provide guidance that should aid in locating specific points of disposal of material which would minimize the threat to the live bottom habitat area.

REFERENCES

- Ackers, P., and White, R. W. 1973. "Sediment Transport: New Approach and Analysis," Journal of the Hydraulics Division, American Society of Civil Engineers, Vol 99, No. HY11, pp 2041-2060.
- Bijker, E. W. 1967. "Some Considerations About Scales for Coastal Models with Movable Bed," Publication No. 50, Delft Hydraulics Laboratory, Delft, The Netherlands.
- Borgman, L. E., and Scheffner, N. W. 1991. "The Simulation of Time Sequences of Wave Height, Period, and Direction," Technical Report DRP-91-2, US Army Engineer Waterways Experiment Station, Vicksburg MS.
- Brandsma, M. G., and Divoky, D. J. 1976. "Development of Model for Prediction of Short-Term Fate of Dredged Material Discharged in the Estuarine Environment," Contract Report D-76-5, US Army Engineer Waterways Experiment Station, Vicksburg MS.
- Ebersole, B. A., Cialone, M. A., and Prater, M. D. 1986. "Regional Coastal Processes Numerical Modeling System; Report 1, RCPWAVE - A Linear Wave Propagation Model for Engineering Use," Technical Report CERC-86-4, US Army Engineer Waterways Experiment Station, Vicksburg MS.
- Jensen, R. E. 1983. "Atlantic Coast Hindcast, Shallow-Water Significant Wave Information," WIS Report 9, US Army Engineer Waterways Experiment Station, Vicksburg, MS.
- Johnson, B. H. 1990. "User's Guide for Models of Dredged Material Disposal In Open Water," Technical Report D-90-5, US Army Engineer Waterways Experiment Station, Vicksburg, MS.
- Johnson, B. H., and Holiday, B. W. 1978. "Evaluation and Calibration of the TETRA TECH Dredged Material Disposal Models Based on Field Data," Technical Report D-78-47, US Army Engineer Waterways Experiment Station, Vicksburg, MS.
- Johnson, B. J., Trawle, M. J., and Adamec, S. A. 1988. "Dredged Material Disposal Modeling in Puget Sound," Journal of Waterways, Port, Coastal, and Engineering, American Society of Civil Engineers, Vol 114, No. 6, pp 700-713.
- Kamphuis, J. W. 1990. "Influence of Sand or Gravel on the Erosion of Cohesive Sediment," Journal of Hydraulic Research, Vol 28, pp 43-53.
- Scheffner, N. W. 1992. "A Dispersion Analysis of the Humboldt Bay, California, Interim Offshore Disposal Site," Miscellaneous Paper DRP-92-1, US Army Engineer Waterways Experiment Station, Vicksburg, MS.
- _____. "Disposal Site Evaluation for the New York Bight," Technical Report (in preparation), US Army Engineer Waterways Experiment Station, Vicksburg, MS.

Scheffner, N. W., and Swain, A. "Evaluation of the Dispersive Characteristics of the Miami and Fort Pierce Dredged Material Disposal Sites," Technical Report (in preparation), US Army Engineer Waterways Experiment Station, Vicksburg, MS.

Swart, D. H. 1976. "Predictive Equations Regarding Coastal Transports," Proceedings of the 15th Coastal Engineering Conference, Honolulu, Hawaii.

Trawle, M. J., and Johnson, B. H. 1986. "Alcatraz Disposal Site Investigation," Miscellaneous Paper HL-86-1, US Army Engineer Waterways Experiment Station, Vicksburg, MS.

White, W. R. 1972. "Sediment Transport in Channels: A General Function," Wallingford Hydraulics Research Station, INT 104, Wallingford, UK.

REPORT DOCUMENTATION PAGE			Form Approved OMB No. 0704-0188	
Public reporting burden for this collection of information is estimated to average 1 hour per response, including the time for reviewing instructions, searching existing data sources, gathering and maintaining the data needed, and completing and reviewing the collection of information. Send comments regarding this burden estimate or any other aspect of this collection of information, including suggestions for reducing this burden, to Washington Headquarters Services, Directorate for Information Operations and Reports, 1215 Jefferson Davis Highway, Suite 1204, Arlington, VA 22202-4302, and to the Office of Management and Budget, Paperwork Reduction Project (0704-0188), Washington, DC 20503.				
1. AGENCY USE ONLY (Leave blank)		2. REPORT DATE March 1994		3. REPORT TYPE AND DATES COVERED Final report
4. TITLE AND SUBTITLE Dispersion Analysis of Charleston, South Carolina, Ocean Dredged Material Disposal Site			5. FUNDING NUMBERS	
6. AUTHOR(S) Norman W. Scheffner James R. Tallent				
7. PERFORMING ORGANIZATION NAME(S) AND ADDRESS(ES) U.S. Army Engineer Waterways Experiment Station 3909 Halls Ferry Road, Vicksburg, MS 39180-6199			8. PERFORMING ORGANIZATION REPORT NUMBER Miscellaneous Paper DRP-94-1	
9. SPONSORING / MONITORING AGENCY NAME(S) AND ADDRESS(ES) U.S. Army Engineer District, Charleston Charleston, SC 29402-0919			10. SPONSORING / MONITORING AGENCY REPORT NUMBER	
11. SUPPLEMENTARY NOTES Available from National Technical Information Service, 5285 Port Royal Road, Springfield, VA 22161				
12a. DISTRIBUTION / AVAILABILITY STATEMENT Approved for public release; distribution unlimited			12b. DISTRIBUTION CODE	
13. ABSTRACT (Maximum 200 words) The dispersive characteristics of the Charleston, SC, Ocean Dredged Material Disposal Site were investigated to determine whether dredging operations could pose a threat to recently discovered live coral reef areas. Two levels of investigation were employed. A short-term analysis of the disposal operation was conducted to examine the immediate fate of material following release from the barge and subsequent descent to the ocean bottom. The second phase examines the long-term fate to determine whether local ocean currents are capable of eroding and transporting deposited material from the site to the reef area. Results of this study indicate the site to be dispersive and recommendations are made as to locations within the designated limits which will minimize the possibility of reef area effect as a result of the disposal operation.				
14. SUBJECT TERMS Disposal site classification Sediment fate Disposal site stability Sediment transport Dredged material			15. NUMBER OF PAGES 76	
			16. PRICE CODE	
17. SECURITY CLASSIFICATION OF REPORT UNCLASSIFIED	18. SECURITY CLASSIFICATION OF THIS PAGE UNCLASSIFIED	19. SECURITY CLASSIFICATION OF ABSTRACT	20. LIMITATION OF ABSTRACT	

Destroy this report when no longer needed. Do not return it to the originator.

